Applied Microbiology and Biotechnology (2019) 103:9037–9055
https://doi.org/10.1007/s00253-019-10119-3

APPLIED MICROBIAL AND CELL PHYSIOLOGY

Cinnamaldehyde inhibits *Candida albicans* growth by causing apoptosis and its treatment on vulvovaginal candidiasis and oropharyngeal candidiasis

Lei Chen[1] · Zhen Wang[1] · Liang Liu[1] · Su Qu[1] · Yuanyuan Mao[1] · Xue Peng[1] · Yong-xin Li[1] · Jun Tian[1,2]

Received: 2 July 2019 / Revised: 21 August 2019 / Accepted: 3 September 2019 / Published online: 28 October 2019

Abstract

The invasion of *Candida albicans* is one of the most common fungal infections seen in clinical practice, and serious drug resistance has been reported in recent years. Therefore, new anti-*C. albicans* drugs must be introduced. In this research, it was demonstrated that cinnamaldehyde (CA) shows strong antimicrobial activity, with 0.26 mg/mL CA being the minimum inhibitory concentration to manage *C. albicans*. Extraordinarily, we detected that CA accumulated the intracellular reactive oxygen species (ROS) and enhanced the calcium concentration in the cytoplasm and mitochondria through flow cytometry. In addition, we observed that *C. albicans* cells released Cytochrome c from the mitochondria to the cytoplasm, depolarized the mitochondrial membrane potential, and activated the metacaspase when exposed to 0.065, 0.13, 0.26, and 0.52 mg/mL CA. Furthermore, to confirm that CA introduces the *C. albicans* apoptosis, we discovered that when the phosphatidylserine was exposed, DNA damage and chromatin condensation occurred, which were detected by terminal deoxynucleotidyl transferase dUTP nick end labeling (TUNEL) and 4′,6-diamidino-2-phenylindole (DAPI) staining. Finally, demonstrations of phenotype investigation, colony-forming unit (CFU) counts, and periodic acid–Schiff (PAS) staining were conducted to prove that CA possessed the ability to treat oropharyngeal candidiasis (OPC) and vulvovaginal candidiasis (VVC). From the above, our research indicates that CA is a promising antifungal candidate when applied to *C. albicans* infections.

Keywords *Candida albicans* · Cinnamaldehyde · Reactive oxygen species · Apoptosis · Vulvovaginal candidiasis · Oropharyngeal candidiasis

Introduction

Candida albicans is a common microbiota in the human oral cavity, upper airway, intestinal tract, and vaginal area; humans with fully functioning immune systems will not be infected by *C. albicans*. Regardless of the rapid development of medical technology, there is a large number of immunosuppressive patients, including those who have undergone an organ transplant and those who have acquired immune deficiency syndrome (AIDS), cancer, and diabetes; in such cases, *C. albicans* can be deadly (Brown et al. 2012). Approximately 10 million cases of thrush occur every year among AIDS patients, neonatal patients, and dentures wearers, and 50% to 75% of women suffer from at least one vulvovaginitis infection during their childbearing stage (Sobel 2007). Furthermore, acquired bloodstream infections caused by *C. albicans* in United States (US) hospitals have resulted in a fatality rate of 40%, and an estimated US$1.7 billion is spent in the US annually in the treatment of such infections (Zaoutis et al. 2005).

The third leading cause of *C. albicans* infection is the use of catheters; 72% of clinical cases of *C. albicans* in Latin America occur because of the use of central venous catheters during hospitalization, and the worldwide mortality rate of catheter-related candidemia has reached 41% (Nucci et al.

Lei Chen and Zhen Wang contributed equally to this work.

✉ Xue Peng
pengxue@jsnu.edu.cn

✉ Yong-xin Li
yongxinli@jsnu.edu.cn

✉ Jun Tian
tj-085@163.com

[1] College of Life Science, Jiangsu Normal University, Xuzhou, 221116 Jiangsu Province, People's Republic of China

[2] Beijing Advanced Innovation Center for Food Nutrition and Human Health, Beijing Technology and Business University, Beijing 100048, People's Republic of China

2013; Wisplinghoff et al. 2004). Nevertheless, while *C. albicans* causes significant clinical distress and economic loss, only a small number of antifungal drugs are available for its treatment; even worse, *C. albicans* is becoming resistant to the current treatments. Against this grim backdrop, there is an urgent need to develop new antifungal drugs with high efficiency and non-toxicity to replace conventional drugs, and novel drug targets are waiting to be discovered to solve the problem of fungal resistance.

At present, scientists are focusing on exploring medicinal plants to develop low-toxicity natural antifungal drugs, as various drug-susceptible or drug-resistant fungi could be inhibited by plants' essential oils (Atanasov et al. 2015; Qu et al. 2019). A natural organic compound called cinnamaldehyde (CA) has been isolated in abundance from the bark of *Cinnamomum cassia*. Cinnamaldehyde is a widely used flavoring agent that has generally been used to improve the taste of food stuffs such as drinks, ice creams, candies, and cachous. CA has also been discovered to treat dyspepsia, gastritis, blood circulation disturbance, and cerebral ischemia through the suppression of TLR4, NLRP3, and NF-κB-dependent inflammation (Liao et al. 2012; Youn et al. 2008; Zhao et al. 2015). In terms of its use as a broad-spectrum antimicrobial, CA has been improved so that it now possesses antibacterial and antifungal abilities, such as in the case of *Pseudomonas aeruginosa*, *Mycobacterium tuberculosis*, and *Salmonella typhimurium* (Burt et al. 2016; Sawicki et al. 2018; Utchariyakiat et al. 2016). In addition, a recent study found that CA has a fungicidal affect on the growth or morphology of *C. albicans* and can inhibit *C. albicans*' mycelial formation (Taguchi et al. 2013).

Apoptosis is a style of cell death. It is critical for the development and homeostasis. During this process, the pro-apoptosis signaling pathways are activated, which in turn activate the caspase proteases and cause mitochondria dysfunction through the specific stimulation of cell stress. When a cell undergoes the apoptosis, characteristic changes occur in the cell morphology, including changes to the roundness of the cell, as blebs occur on the plasma membrane and nuclear fragmentation occurs (Degterev and Yuan 2008). Our group has shown that apoptosis is an important target of antifungal drugs (Tian et al. 2018). Therefore, in the present study, we sought to explore the mechanism by which cinnamaldehyde inhibits *C. albicans* and the therapeutic effects that occur in a mouse model of oropharyngeal candidiasis (OPC) and vulvovaginal candidiasis (VVC).

Material and methods

Strains and agent

C. albicans American Type Culture Collection (ATCC) 64547 was obtained from the American Type Culture Collection (ATCC; Manassas, VA, USA) and was used in vitro. The clinical *C. albicans* (09-1555) which was used in animal experiment was isolate obtained from a patient with recurrent vulvovaginal candidiasis. The test fungal strain was maintained in Sabouraud Dextrose Broth (SDB) medium (1% peptone, 4% dextrose) at 37 °C overnight. The CA (CAS Registry No. 104-55-2) used in this research was purchased from Shanghai Macklin Biochemical Co., Ltd. (Shanghai, China) and hydrogen peroxide (H_2O_2) used in this study was purchased from Sigma-Aldrich. It was diluted to concentrations of 0, 0.065, 0.13, 0.26, and 0.52 mg/mL CA using 0.1% (*v*/*v*) Tween-80.

Animals

Six-week-old male and female BALB/c mice were purchased from the Institute of Experimental Animals, Chinese Academy of Medical Sciences (Beijing). All mice were grouped at a specific pathogen-free (SPF) facility with a controlled temperature of 22–24 °C, a relative humidity of 60%, and a 12 h/12 h light–dark cycle. All animal experiments were conducted in accordance with the Chinese legislation on the use and care of laboratory animals. The protocol was authorized by the Jiangsu Normal University Committee for Animal Experiments to minimize the suffering of the mice used. All animal experiments were proceeded in Jiangsu Normal university IVC animal experiment platform.

Test of antifungal susceptibility

The method for determining the minimum inhibitory concentration (MIC) was used as previously reported (Tian et al. 2017b). First, we added 100 μL of SDB medium to each well in a sterile 96-well microtiter plate. Then, 80 μL of CA solution was added to each well and serially diluted two-fold, resulting in final concentrations of CA ranging from 0.016 to 4.16 mg/mL. In addition, two wells were treated as the blank and negative growth control wells, without the addition of CA. Finally, yeast cells of *C. albicans* were adjusted to 10^6 CFU/mL by phosphate-buffered saline (PBS, pH = 7.4), and the diluent (20 μL/well) was added to each well. After incubation at 37 °C for 24 h, the MIC that inhibited the growth of the *C. albicans* were identified through 80 ng/μL resazurin using visual observation.

Measurement of intracellular ROS

C. albicans cells were cultured in a conical flask and adjusted to 5×10^6 cells/mL using sterile PBS. Then, the cells were treated for 8 h at 37 °C with 0, 0.065, 0.13, 0.26, and 0.52 mg/mL CA. In addition, according to the previous research, H_2O_2 has been proved to be a well-known apoptosis inducer and can disrupt the mitochondria membrane, so we

used 0.3 mg/mL H_2O_2 as the positive control (Madeo et al. 1999; Phillips et al. 2003). The drug was discarded after a 5000*g* centrifuge for 5 min. The cells were washed twice using PBS, and then incubated with 10 μM DCFH-DA for 30 min at 37 °C to detect the levels of intracellular ROS. Finally, the cells were washed twice using PBS and analyzed with an Accuri C6 flow cytometer (BD Biosciences, San Jose, CA, USA).

Assay of calcium ions in cytoplasm and mitochondrion

The effect of CA on Ca^{2+} in the cytoplasm and mitochondrion of *C. albicans* were analyzed using Fluo-3/AM and Rhod-2/AM, respectively. Briefly, fresh *C. albicans* cells were diluted to 5×10^6 cells/mL and incubated with 0, 0.065, 0.13, 0.26, 0.52 mg/mL CA and 0.3 mg/mL H_2O_2 at 37 °C for 8 h. Then, the cells were washed twice using PBS, and the Fluo-3/AM and Rhod-2/AM were incubated with *C. albicans* cells at 37 °C for 30 min. Before testing, the probe was cleaned out using PBS and detected using an Accuri C6 flow cytometer (BD Biosciences, San Jose, CA, USA).

Detection of mitochondrial membrane potential ($\Delta\psi_m$)

The $\Delta\psi_m$ detection was performed according to a method published in a previous report (Alonso-Monge et al. 2009). *C. albicans* cells were re-suspended to 5×10^6 cells/mL and exposed to various concentrations of CA (0, 0.065, 0.13, 0.26, 0.52 mg/mL) and 0.3 mg/mL H_2O_2 at 37 °C for 8 h. Then, the *C. albicans* cells were harvested by centrifuge by 5000*g* for 5 min, washed twice, and incubated in 10 μg/mL of JC-1 solution for 0.5 h at 37 °C. After washing twice with PBS, the $\Delta\psi_m$ was analyzed using an Accuri C6 flow cytometer (BD Biosciences, San Jose, CA, USA).

Western blotting analysis of the release of cytochrome c

In brief, the *C. albicans* cells were disposed to 0, 0.065, 0.13, 0.26, 0.52 mg/mL CA and 0.3 mg/mL H_2O_2 at 37 °C for 8 h. Then, the cells were collected, and the mitochondrial protein or cytoplasm protein was extracted using a fungal mitochondrial protein extraction kit (BestBio, China). The 50-μg protein samples were separated using sodium dodecyl sulfate polyacrylamide gel electrophoresis (SDS-PAGE) denatured gel and transferred to a polyvinylidene difluoride membrane (Merck Millipore, Billerica, MA, USA). The membranes were blocked with 5% nonfat milk dissolved in Tris-buffered saline containing 0.1% Tween-20 (TBST) and incubated at 4 °C overnight with rabbit anti-cytochrome c and mouse anti-GAPDH (Proteinsimple, USA) antibodies. Then, the horseradish peroxidase (HRP)-linked goat anti-rabbit or anti-mouse secondary antibodies were incubated at room temperature for 40 min and washed using TBST. The protein expression levels of cytochrome c were detected using enhanced chemiluminescence substrate.

Measurement of metacaspase activity

The change of metacaspase activation in *C. albicans* after treatment with CA was measured using CaspACE FITC-VCD-FMK. In brief, the *C. albicans* cell suspensions—adjusted to 5×10^6 cells/mL in sterile PBS—were combined with different concentrations of CA (0, 0.065, 0.13, 0.26, 0.52 mg/mL) and 0.3 mg/mL H_2O_2 at 37 °C. After incubation for 8 h, the cells were washed twice using PBS, re-suspended in 500 μL of staining solution containing 5 μg/mL of CaspACE FITC-VCD-FMK, and incubated for 30 min at room temperature in the dark. Finally, the samples were tested using an Accuri C6 flow cytometer (BD Biosciences, San Jose, CA, USA).

Double staining analysis of PS externalization

We used Fourier-infrared transform chromatography (FITC) coupled with Annexin V reaction, using the Annexin V-FITC kit from BD Biosciences (San Jose, USA), to analyze the externalization extent of PS. The detection of PS externalization was based on *C. albicans* protoplasts. The *C. albicans* protoplasts were achieved using 1 M sorbitol, 1.5% Snailase, and 0.1 M PBS solution, incubated at 37 °C for 2 h. Thereafter, protoplasts were collected after 5000*g* centrifuge for 10 min and resuspended using washing buffer (1 M sorbitol, 0.8 M NaCl, 10 mM $CaCl_2$, and 50 mM Tris-HCl; pH = 7.5). Then, 5×10^6 cells/mL *C. albicans* protoplasts were incubated with 0, 0.065, 0.13, 0.26, 0.52 mg/mL CA and 0.3 mg/mL H_2O_2 at 37 °C for 4 h and 8 h. The treated cells were stained using 5 μL/mL propidium iodide and 5 μL of Annexin V-FITC at room temperature for 30 min in the dark. Finally, the stained protoplasts were detected using an Accuri C6 flow cytometer (BD Biosciences, San Jose, CA, USA).

DNA damage and nuclear fragmentation assay

DNA damage and nuclear fragmentation are significant markers of apoptosis. In this study, we used DAPI and TUNEL staining to evaluate the nuclear condensation and DNA strand breaks. Briefly, for TUNEL and DAPI staining (Solarbio, China), the treated *C. albicans* cells were fixed in a glass slide using 4% paraformaldehyde and 70% ethanol and washed using sterile PBS. Afterwards, the cells were labeled with a cell death detection kit for 1 h at 37 °C and 5 μg/mL DAPI. Finally, the glass slides were viewed using a fluorescence microscope (Leica, Germany).

Murine models of OPC and VVC

The murine models of OPC and VVC were established according to the previous reports described, with some alterations (Conti et al. 2009). All mice were divided to six groups with 12 per each group, given specific amounts of food for a week, as follows:

Wild-type (WT) mice were given normal chow, were given the same amounts of anesthesia, and were not invaded by *C. albicans* on the infection day; they were washed daily using the vehicle (0.1% [*v/v*] sterile Tween-80) at the same time as one another.

Control mice were given normal chow, were invaded by *C. albicans* with no treat, and were washed daily with the vehicle (0.1% [*v/v*] sterile Tween-80) at the same time.

In addition, VVC mice were treated by 0.52, 1.04, 1.56 mg/kg CA and 20 mg/kg fluconazole (FCZ), and OPC mice were treated by 1.3, 2.6, 3.9 mg/kg CA and 20 mg/kg FCZ.

For the OPC, on the first day before infection and the first and third days after infection, male mice were immunosuppressed by intramuscular injection cortisone acetate (225 mg/kg) (Solis et al. 2017). On the infection day, mice were narcotized by urethane (1.25 mg/kg, intraperitoneal injection), and the tongues were lightly scraped using a bistoury, without causing bleeding. Small cotton pellets, saturated with 100 μL *C. albicans* cells (6×10^8 cells/mL), were placed in the oral cavity while the mice were under anesthesia for 2 h. After the infection of *C. albicans*, the mice were rinsed by CA and FCZ once a day for consecutive 5 days. The mice were killed on day 6 and the tongues and other organs were harvested by surgical scissors. The clinical score of tongue was referenced a previous reported scoring system (Hise et al. 2009).

For the VVC, female mice were subcutaneous through the use of 0.2 mg estradiol benzoate every other day for three times in a week. Mice were narcotized with 1.25 mg/kg urethane and inoculated with 20 μL of 6×10^8 cells/mL *C. albicans* cells into the vaginal lumen. One day after infection, vaginal lavages were performed on the mice using 500-μL sterile PBS and the diff-quick strain lavage fluids were assessed. After the accomplishment of the murine model, the mice vaginas were douched with various concentrations of CA and 20 mg/kg FCZ every day in the same time by mechanical pipette into the vaginal lumen for consecutive 5 days. The mice were sacrificed at day 6 and the vaginas were harvested by surgical scissors cautiously.

After obtaining tissue, the tongue and vagina were fixed with 4% paraformaldehyde, and then frozen sections were used for hematoxylin and eosin staining (HE) and periodic acid schiff staining (PAS) staining. For fungal burden assay, the tissue was added to sterile PBS and disrupted with a homogenizer, and then, 5% tissue homogenate was added to the culture medium containing chloromycin in SDA medium. Colony count after 2 days of culture at 37 °C.

Statistical analysis

All data were obtained from at least three independent experiments. The data were presented as means ± standard deviation and were all analyzed using a one-way ANOVA, as appropriate, using GraphPad Prism software, version 5.01. Statistical significance was set at $p < 0.05$ for all tests.

Results

Antimicrobial activity of CA against *C. albicans*

In this study, 0.065, 0.13, 0.26, and 0.52 mg/mL CA were the concentrations selected to be investigated in relation to the antimicrobial mechanism of CA against *C. albicans*. The minimum inhibitory concentration (MIC) of CA against *C. albicans* was assessed during 5 days of co-incubation by visual observation. As shown in Fig. 1, the growth of *C. albicans* was significant at the lower concentration of 0.065 mg/mL CA but was almost completely suppressed at 0.13 mg/mL CA, when compared to the growth in the 0 mg/mL CA-treated group and blank group. Given these observations, the MIC of CA to inhibit the growth of *C. albicans* was shown to be 0.13 mg/mL.

Accumulation of reactive oxygen species (ROS) in *C. albicans* cells introduced by CA

Previous studies have proposed that the potential mechanisms of apoptosis-mediated biofilm damage in CA-treated *C. albicans* are associated with a release of cytochrome c. Notably, cytochrome c released from the mitochondria to the cytosol was a classic sign of apoptosis. ROS have been confirmed to be a consequence of cellular oxygen metabolism, and their accumulation is suggested to be a marker of apoptosis in *Aspergillus flavus* (Aguirre et al. 2005). Thus, we investigated the production of intracellular ROS using the sensitive

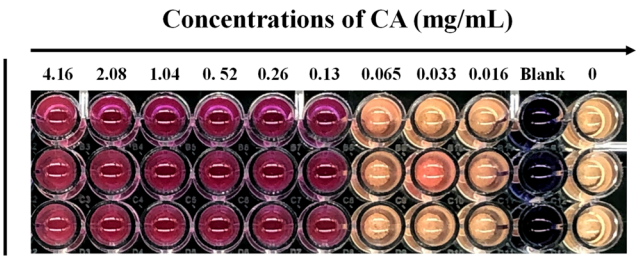

Fig. 1 The MIC of *C. albicans* cells inhibited by CA using the microdilution method, with the endpoints observed using resazurin

fluorescent dye 2′,7′-dichlorofluorescein diacetate (DCFH-DA) by flow cytometer and fluorescence microscope. Our results showed that CA enhanced ROS production in a concentration-dependent manner at various concentrations of CA (0, 0.065, 0.13, 0.26, 0.52 mg/mL) and 0.3 mg/mL H_2O_2. According to the flow cytometer, the intracellular ROS production occurred at rates of 2.7% ± 2.52%, 7.4% ± 4.21%, 16.1% ± 8.43%, 28.9% ± 8.49%, 55.2% ± 16.23%, and 24.68% ± 2.91%, respectively, and the results were consistent with those of the fluorescence microscope (Fig. 2a and b). In addition, our results indicated that CA can introduce more ROS than H_2O_2 in *C. albicans* when cells were exposed to a nearly concentration. This data indicated that CA promoted the accumulation of intracellular ROS.

Effect of CA on cytoplasm and mitochondria Ca^{2+}

Another crucial regulator of cell survival and apoptosis in response to various cellular signals is Ca^{2+} release from the mitochondria (Giacomello et al. 2007). In this study, Fluo-3/AM and Rhod-2/AM stains were used to detect the levels of Ca^{2+} in the *C. albicans* cytoplasm and mitochondria. As shown in Fig. 3a, the flow cytometer assay showed that the Fluo-3/AM fluorescence intensities were 2.8 ± 0.34%, 5.24 ± 1.37%, 10.16 ± 1.16, 21.24 ± 6.29%, 35.87 ± 4.24%, and 28.6% ± 2.66% in cytoplasm after it was treated with various concentrations of CA (0.065, 0.13, 0.26, 0.52 mg/mL) and 0.3 mg/mL H_2O_2, respectively. In addition, after the application of different concentrations of CA, the Ca^{2+} in mitochondria were increased: in the group treated with 0.52 mg/mL CA, it was increased to 71.35 ± 5.24%, meaning the Ca^{2+} content in mitochondria was double that in the cytoplasm and 0.3 mg/mL H_2O_2 showed strong destructive effects on mitochondria (Fig. 3b). Furthermore, the results gathered through the fluorescence microscope corresponded with those gathered through the flow cytometer (Fig. 3c and d). These results indicated that CA mediated the release of Ca^{2+} in *C. albicans*.

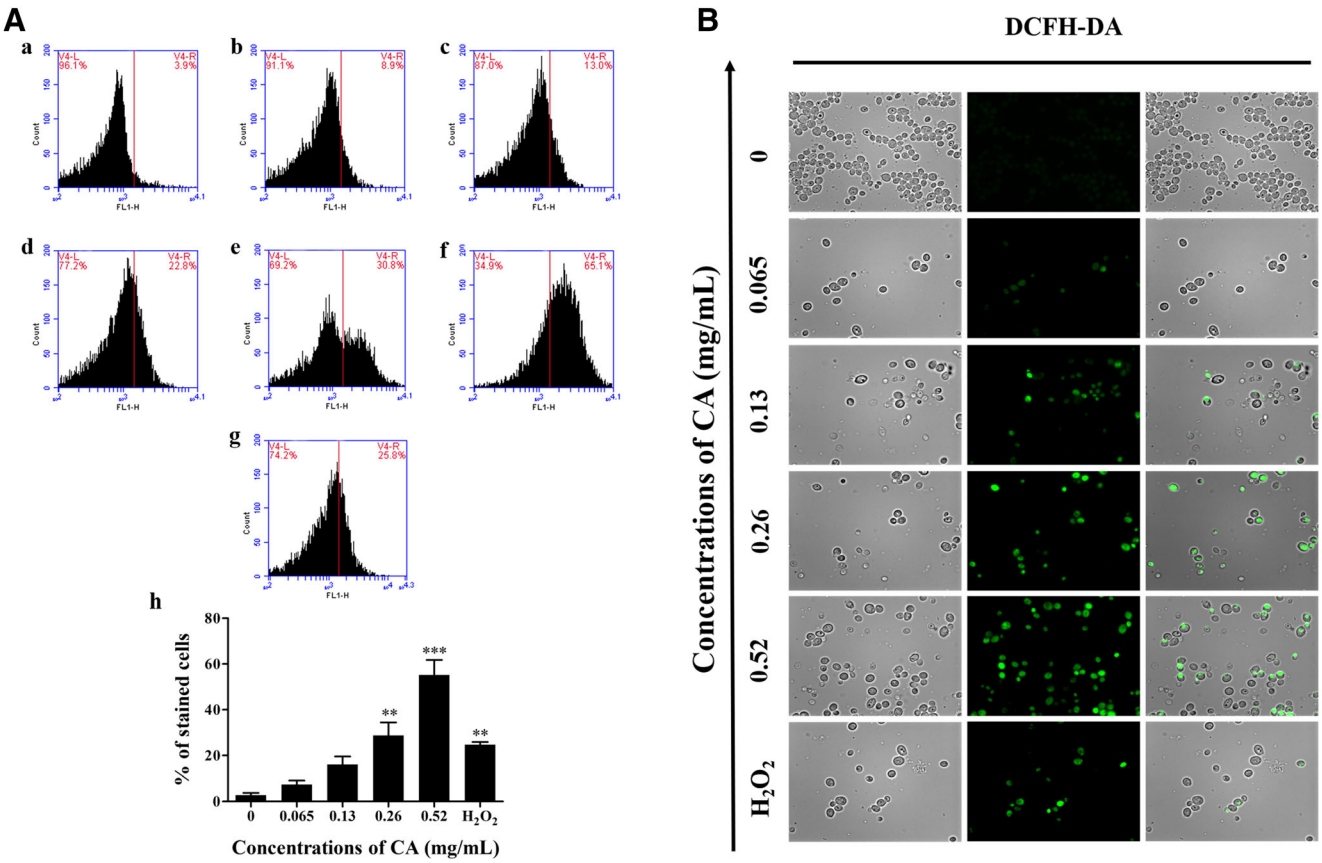

Fig. 2 The accumulation of intracellular ROS after *C. albicans* was co-incubated with various concentrations of CA. **A** Flow cytometry analysis of intracellular ROS content through DCFH-DA: **a** non-treated cells' autofluorescence, **b** cells treated with fluorescence dye, **c**–**g** *C. albicans* cells disposed to 0.065, 0.13, 0.26, 0.52 mg/mL CA and 0.3 mg/mL H_2O_2, **h** statistical analysis of stained cells' percentages; $^{**}p < 0.01$ and $^{***}p < 0.001$ when compared with the 0 mg/mL CA group. **B** The levels of ROS in *C. albicans* cells treated by various concentrations of CA, detected by fluorescence microscope through DCFH-DA

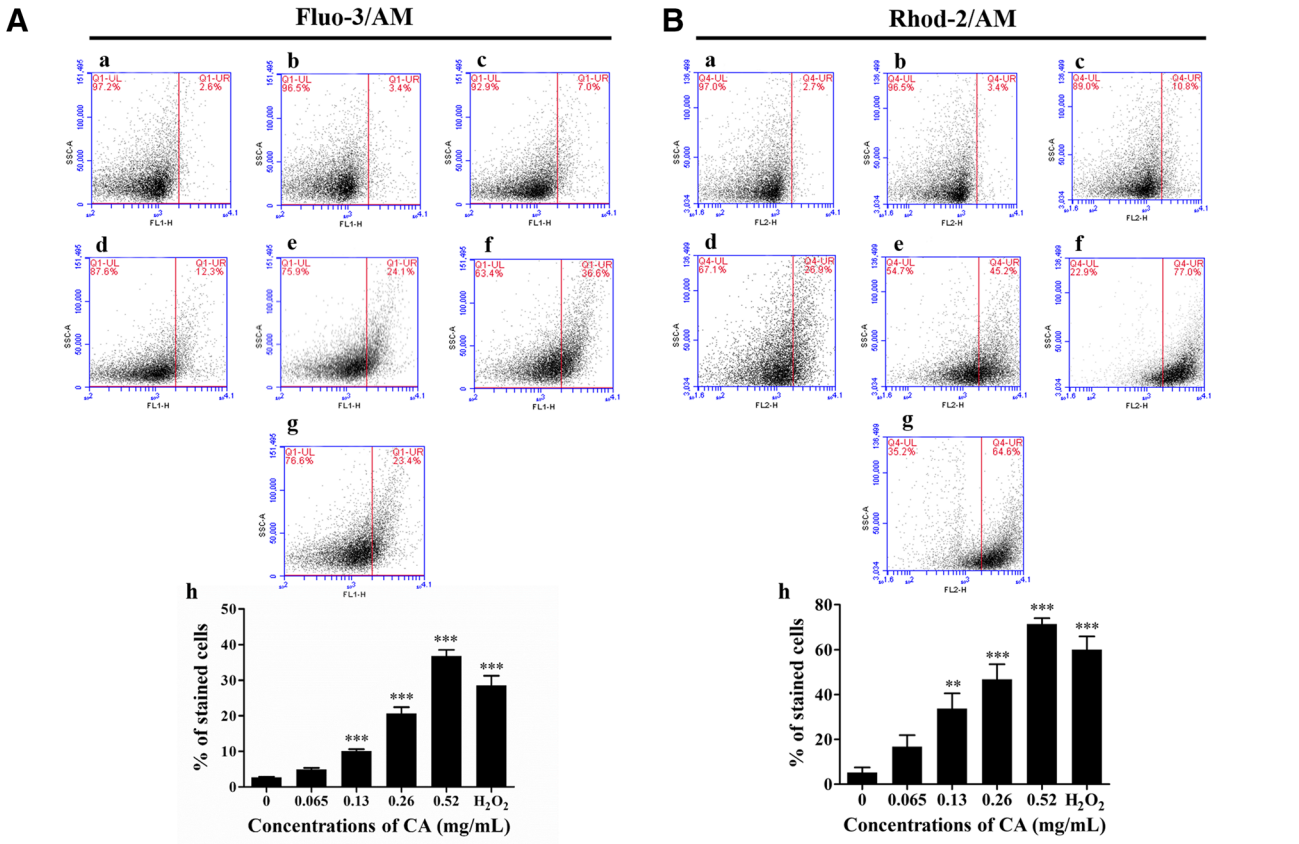
A
Fluo-3/AM
a
b
c
d
e
f
g
h
% of stained cells
Concentrations of CA (mg/mL)
0
0.065
0.13
0.26
0.52
H2O2
B
Rhod-2/AM
a
b
c
d
e
f
g
h
% of stained cells
Concentrations of CA (mg/mL)
0
0.065
0.13
0.26
0.52
H2O2

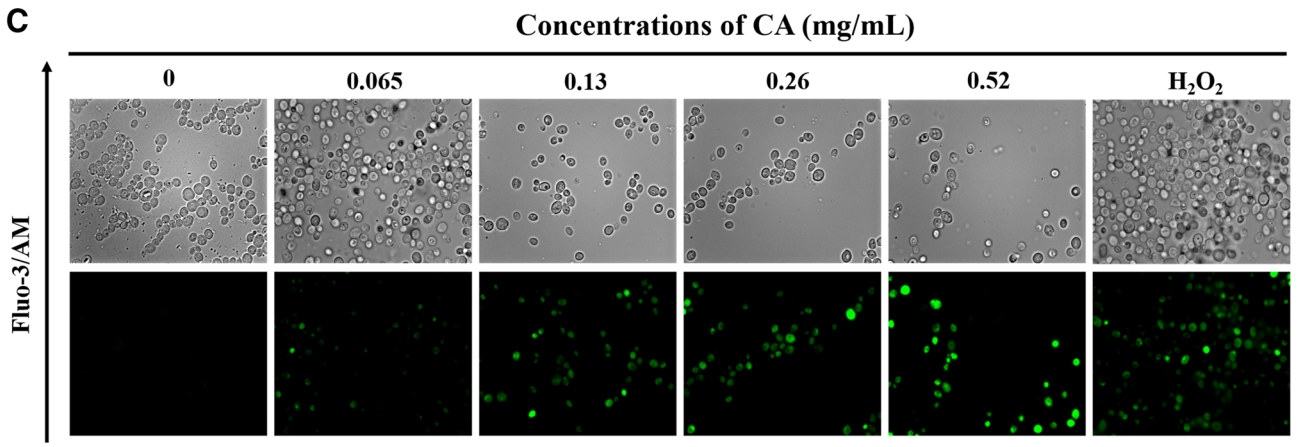
C
Concentrations of CA (mg/mL)
0
0.065
0.13
0.26
0.52
H2O2
Fluo-3/AM

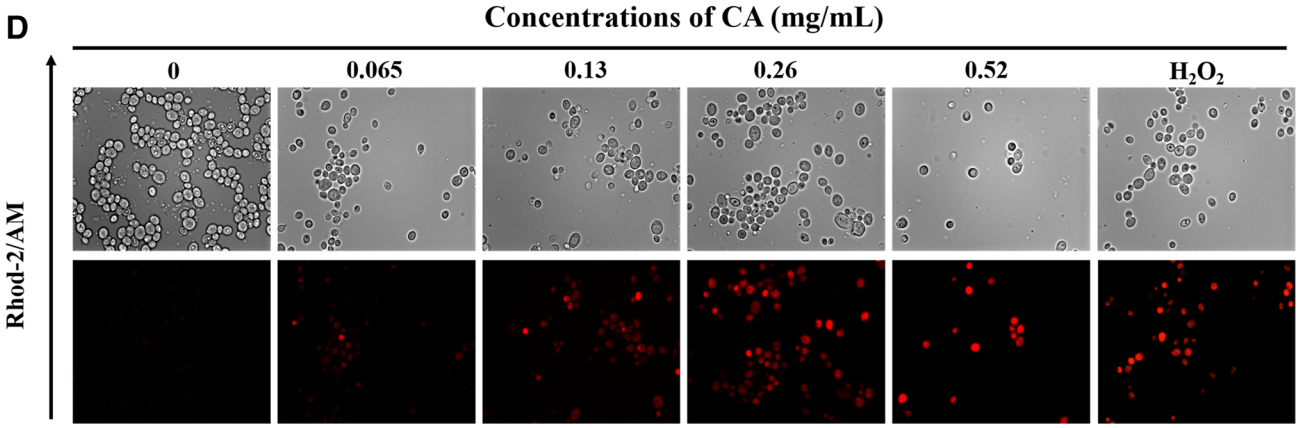
D
Concentrations of CA (mg/mL)
0
0.065
0.13
0.26
0.52
H2O2
Rhod-2/AM

◀ **Fig. 3** CA treatment leads to an increase in the calcium levels of *C. albicans* cells' mitochondria and cytoplasm. **A** The calcium levels in the cytoplasm were detected by Fluo-3/AM through flow cytometry: **a** the autofluorescence of *C. albicans* cells, **b–g** cells treated with fluorescence dye, 0, 0.065, 0.13, 0.26, 0.52 mg/mL CA and 0.3 mg/mL H_2O_2, **h** a histogram of the calcium levels in the cytoplasm. **B** The calcium levels in the mitochondria were detected by Rhod-2/AM through flow cytometry: **a** the auto fluorescence of *C. albicans* cells, **b–g** cells treated with th fluorescence dye, 0, 0.065, 0.13, 0.26, 0.52 mg/mL CA and 0.3 mg/mL H_2O_2, **h** a histogram of the calcium levels in the mitochondria. **C** Fluorescence microscope detected the calcium levels in the cytoplasm through fluorochrome Fluo-3/AM. **D** Fluorescence microscope detected the calcium levels in the mitochondria through fluorochrome Rhod-2/AM. In all statistical analysis, $^{**}p < 0.01$ and $^{***}p < 0.001$, compared with the 0-mg/mL CA group

Depolarization of the mitochondrial membrane potential through CA

$\Delta\psi_m$ is a very sensitive marker of the energy-coupling condition of mitochondria, and it was affected by the accumulation of ROS (Kuang et al. 2017). Therefore, the flow cytometer and fluorescence microscope were used to detect changes in the $\Delta\psi_m$ in *C. albicans* after CA treatment. As shown in Fig. 4a, the $\Delta\psi_m$ was decreased to 52.98 ± 10.79%, 40.31 ± 7.43%, 40.21 ± 4.44%, 39.65 ± 3.65%, and 46.1% ± 2.92% (with the application of 0.065, 0.13, 0.26, 0.52 mg/mL CA and 0.3 mg/mL H_2O_2, respectively) compared with the untreated group (69.83 ± 3.86%). Per examination under the fluorescence microscope, the 0- and 0.065-mg/mL CA-treated groups showed red fluorescence because of high levels of $\Delta\psi_m$, which lead to polymerized JC-1 staining in the mitochondria. Nevertheless, the *C. albicans* disposed by 0.13, 0.26, 0.52 mg/mL CA and 0.3 mg/mL H_2O_2 exhibited more green fluorescence due to the decreased $\Delta\psi_m$, which resulted in dispersed JC-1 staining in the mitochondria (Fig. 4b). These results indicated that CA can decrease the level of $\Delta\psi_m$ in *C. albicans* cells in a concentration-dependent manner.

Release of cytochrome c through CA treatment

One of the typical markers of apoptosis is the release of cytochrome c from the mitochondria to the cytoplasm (Wang and Youle 2009). In our research, we utilized Western blotting to detect the intracellular change of cytochrome c. As shown in Fig. 5, after *C. albicans* cells co-incubated with various concentrations of CA, the cytochrome c was significantly reduced in mitochondria and the expression levels in the cytoplasm were significantly enhanced when compared with those of the control group. When compared with 0.3-mg/mL H_2O_2-treated cells, 0.13 mg/mL CA exhibited similar effects. This result indicates that CA induces cytochrome c release from the mitochondria to the cytoplasm in *C. albicans* cells.

Effect of CA on metacaspase activation

In general, the caspase family plays a central role in apoptosis in humans, and metacaspases are caspase-like cysteine proteases associated with the accumulation of ROS and mitochondrial dysfunction in fungal cells (Fuchs and Steller 2011). As shown in Fig. 6, the cells were stained with FITC-VAD-FMK and incubated with 0, 0.065, 0.13, 0.26, 0.52 mg/mL CA and 0.3 mg/mL H_2O_2; the fluorescence intensity was observed to range from 5.83 ± 2.19 to 61.94 ± 16.22%. In addition, we observed that the activity of metacaspases was increased to 50.8 ± 2.19% at 0.26 mg/mL CA; in contrast, the activity occurred at a level of 21.01 ± 7.03% in the group treated with 0.13 mg/mL CA and 32.27% ± 4.17% treated with and 0.3 mg/mL H_2O_2. This result showed that CA activated the metacaspases to induce apoptosis in *C. albicans*.

CA leads to phosphatidylserine (PS) externalization

In mammalian and fungal cells, the externalization of PS translocated from the inner surface to the outer leaflet is a classic early indicator of apoptosis (Madeo et al. 1997). In this study, we utilized the Annexin V-FITC and propidium iodide (PI) double staining to distinguish the apoptotic and necrotic cells. As shown in Fig. 7a, after exposure to different concentrations of CA (0, 0.065, 0.13, 0.26, and 0.52 mg/mL) and 0.3 mg/mL H_2O_2 for 4 h, the percentage of early apoptotic cells reached 3.49 ± 0.39%, 5.43 ± 0.52%, 9.61 ± 3.05%, 16.91 ± 3.41%, 29.64 ± 7.21%, and 13.07% ± 1.67%, respectively. Afterwards, we detected the externalization of PS under the treatment at various concentrations of CA for 8 h; the externalization of PS showed an obvious time–dose-dependent relationship. The ratio of Annexin V-positive and PI-negative cells was 6.9 ± 1.51%, 12.68 ± 3.6%, 16.54 ± 0.73%, 40.55 ± 11.26%, 56.83 ± 1.85%, and 21.2% ± 2.29%. These data conclusively exhibit that CA-mediated apoptosis in a time–dose-dependent manner in *C. albicans* cells.

DNA damage and chromatin condensation introduced by CA

DNA damage and chromatin condensation, which are hallmarks of apoptosis, were detected using 4′,6-diamidino-2-phenylindole (DAPI) and terminal deoxynucleotidyl transferase dUTP nick-end labeling (TUNEL). The fluorescence microscope results indicated that the nuclear morphology appeared to be more fragmented, and greater fluorescence intensity was seen when compared to that of the group treated with 0 mg/mL CA. Furthermore, the positive-signaling fluorescence degree was enhanced as the concentration of the drug increased (Fig. 7d). Therefore, after treatment at various concentrations CA, *C. albicans* cells exhibited DNA damage and chromatin condensation, which are markers of later apoptosis.

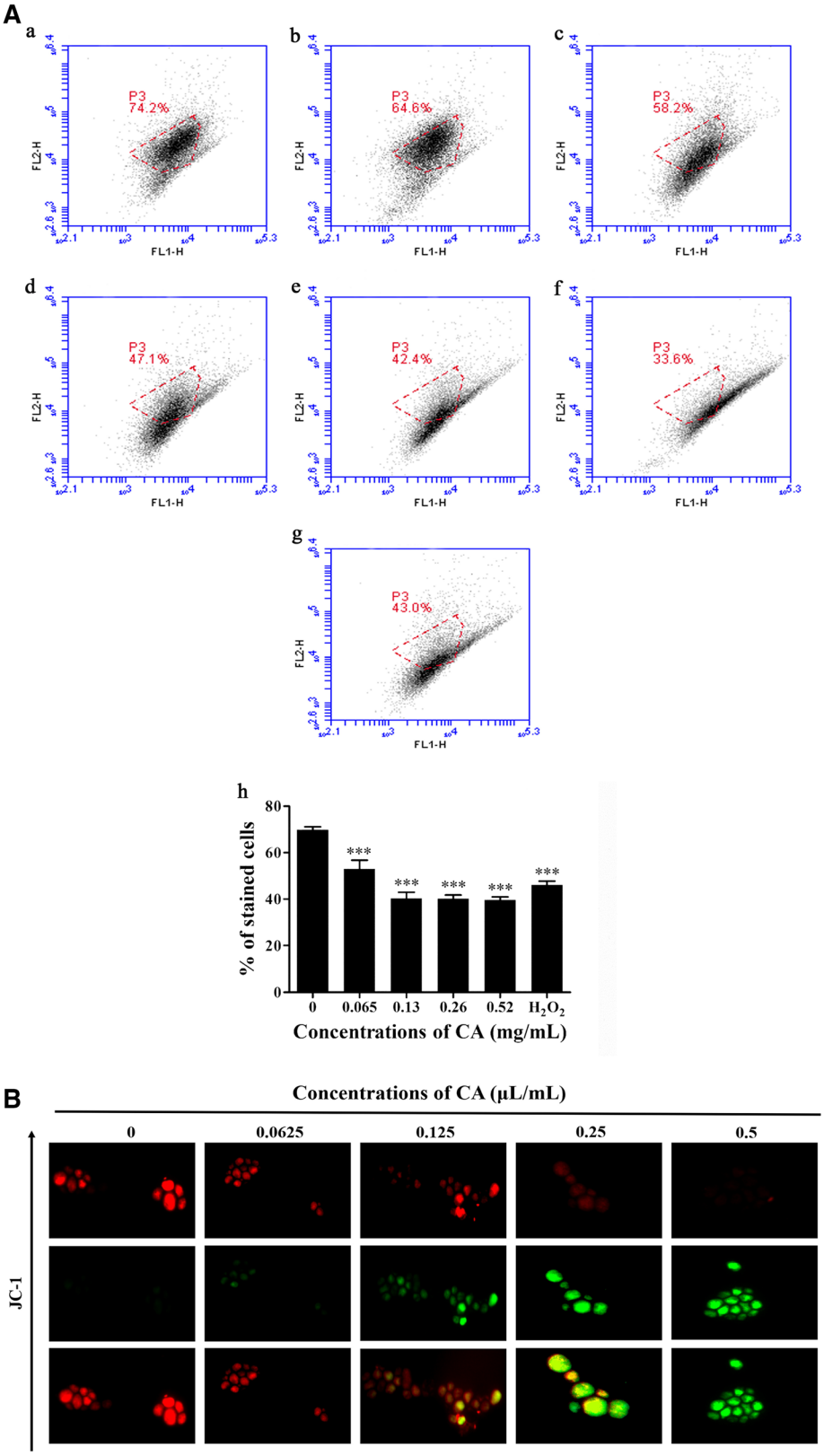

Fig. 4 The mitochondrial membrane potential was depolarized in *C. albicans* cells because of exposure to various concentrations of CA. **A** The detection of Δψm in cells was analyzed using flow cytometry: **a** the autofluorescence of non-treated cells. **b–g** cells treated with 0, 0.065, 0.13, 0.26, 0.52 mg/mL CA and 0.3 mg/mL H_2O_2. **h** a one-way analysis of variance (ANOVA) in the detection of Δψm; ***$p < 0.001$, compared with the 0-mg/kg CA-treated group. **B** A fluorescence microscope analyzed the variation in Δψm, with red fluorescence indicating high Δψm and green fluorescence indicating low Δψm in *C. albicans*

CA improved the condition of VVC in vivo

To confirm whether the in vitro activity of CA against *C. albicans* is also displayed in vivo, we evaluated the efficacy of CA in an experimental murine model of VVC. The mice were executed at day 6 after infection, and the change in *C. albicans* invasion was detected using Diff quick staining. The staining results, reported in Fig. 8a, demonstrated that mainly epithelial cells and, rarely, immune cells were shown in the vaginal fluid of uninfected mice. In contrast, in infected mice, various cell types were observed in staining, and most of them were neutrophils.

To quantify the damage of the vaginitis, we plated the vaginal tissues on sabouraud dextrose agar (SDA) and cultured them to assess the level of mice vaginal *C. albicans* according to colony-forming unit (CFU) count. As shown in Fig. 8b, uninfected mice had a low fungal burden of *C. albicans*, and 0.52-mg/kg CA-treated mice and 20-mg/kg CA-treated mice also possessed low levels of fungal burden ($p > 0.05$). Nevertheless, *C. albicans*-invaded mice that did not receive treatment contained nearly 100-fold the fungal burden when compared with the WT group ($p < 0.001$) and a remarkable difference when compared to the 0.52-mg/kg CA and 20-mg/kg fluconazole (FCZ)-treated groups ($p < 0.01$). The 1.04- and 1.56-mg/kg CA-treated groups also showed significant differences when compared to the WT group ($p < 0.01$).

Interestingly, in the course of our dissection, we discovered that in mice that were not infected with *C. albicans*, the uterus and fallopian tubes appeared milky and smooth. However, the infected mice that received no treatment showed serious inflammation in the ovaries, fallopian tubes, and uterus; these organs appeared transparent and were severely swollen. In addition, mice treated with 1.04 mg/kg CA, 1.56 mg/kg CA, and 20 mg/kg CA showed obvious improvement in the uterus, as the swelling was slowly subsiding; in the group treated with 0.52 mg/kg CA, the swelling had almost been reduced to a normal level (Fig. 8c).

Based on these results, we initially thought that 0.52 mg/kg CA may be the most suitable dosage to improve VVC. As such, we used histochemical stain on a frozen section to confirm the optimal dose for the treatment of vaginitis in mice. Our periodic acid–Schiff (PAS) staining results indicated that the vaginas of the control group mice were full of red hypha, exhibiting serious inflammation, with a large number of neutrophils extracted. In contrast, the group treated with 0.52 mg/kg CA and 20 mg/kg FCZ possessed a relatively complete organizational structure and fewer *C. albicans* cells in vaginas. However, the groups treated with 1.04 and 1.56 mg/kg CA exhibited more fungus and tissue damage than did the group treated with 0.52 mg/kg CA, as well as less injury than that seen in the control group (Fig. 8d). As such, we confirmed that CA can be used to treat VVC in vivo and

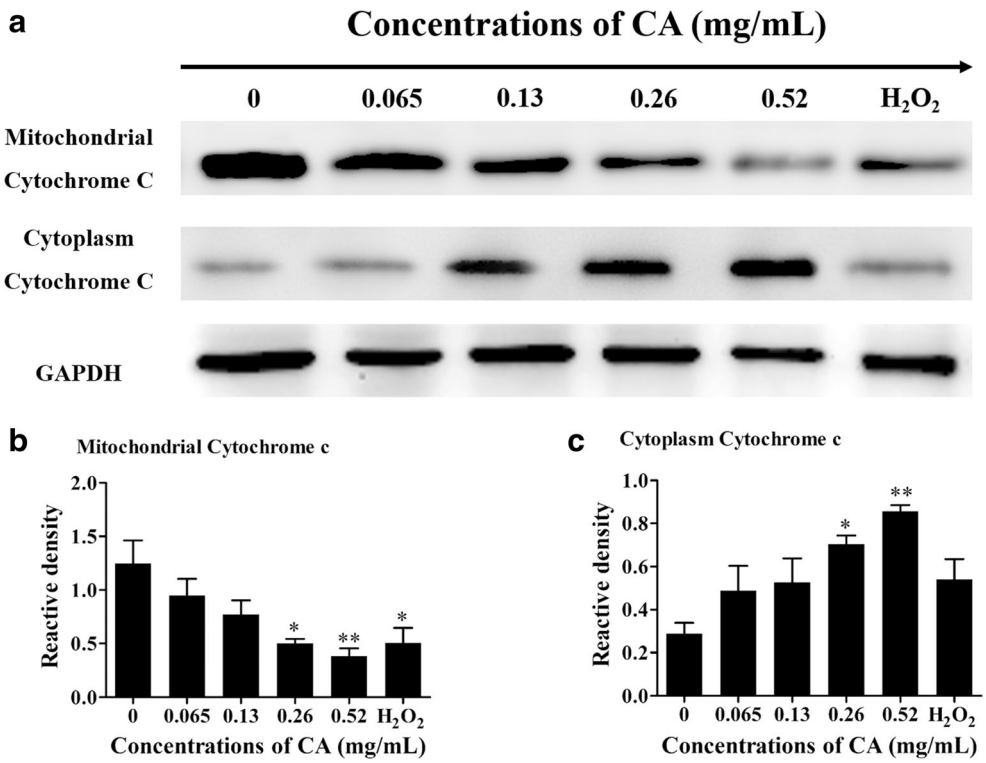

Fig. 5 CA introduced the release of cytochrome c from the mitochondria to the cytoplasm. **A** Western blotting was used to analyze the expression of cytochrome c in the mitochondria and cytoplasm. **B** The reactive density of the cytochrome c content in mitochondria. **C** The reactive density of the cytochrome c content in the cytoplasm. In all statistical analysis, $*p < 0.05$, $**p < 0.01$, compared with the 0-mg/mL CA group

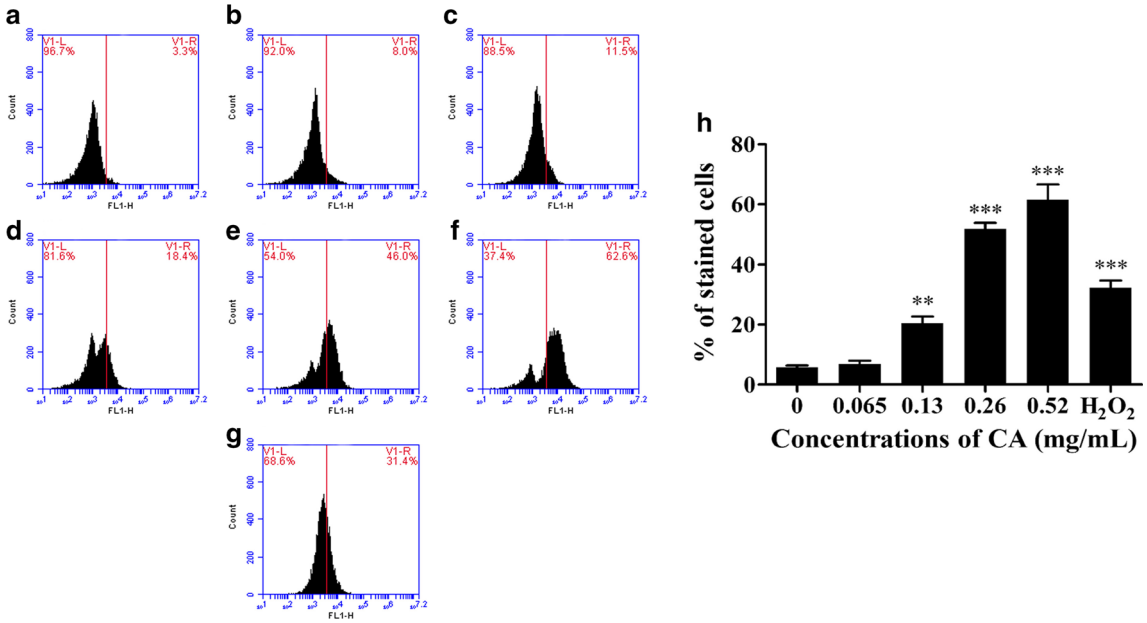

Fig. 6 CA introduced apoptosis in *C. albicans* cells through the metacaspase pathway. **A** Autofluorescence in *C. albicans* cells. **B–G** *C. albicans* cells were exposed to 0, 0.065, 0.13, 0.26, 0.52 mg/mL CA and 0.3 mg/mL H_2O_2 and measured using flow cytometry. **H** Statistical analysis of metacaspase-active cells; $^{**}p < 0.01$ and $^{***}p < 0.001$, compared with the 0-mg/mL CA group

suggest that 0.52 mg/kg CA is the optimal dose to treat vaginitis caused by *C. albicans*.

CA is effective against OPC in vivo

The potential therapy effect of CA as a topical protective for OPC was tested using a murine model of OPC. We discovered that at the end of molding (day 5), tongue phenotypes of CA-treated mice had significantly smaller amounts of white plaque that did untreated mice, as well as reduced colonization and invasion on mouse tongues, according to visual analysis (Fig. 9a). The clinical score of the degree of infection found in mouse tongues was evaluated with reference to a previous report (Hise et al. 2009), as shown in Fig. 9b; the fungal burden scores of tongues from WT mice and 3.9-mg/kg CA-treated mice were significantly lower than the control group mice ($p < 0.001$). In addition, we discovered that changes in mouse body weight and survival rate were exhibited in relation to the dosage, with mice treated with 3.9 mg/kg CA possessing the highest survival rate and lowest rate of body weight loss after infected by *C. albicans* (Fig. 9c and d).

To better illustrate the therapeutic dose of CA, we quantitated the amount of fungus in mouse tongues and viscera using CFU counting. As shown in Fig. 9e and f, the *C. albicans* burden of the WT group and 3.9-mg/kg CA-treated group were also obviously decreased when compared to the control group, 1.3 mg/kg CA, and 2.6-mg/kg CA-treated group ($p < 0.05$), and there was no distinct difference between the WT group and 3.9-mg/kg CA-treated group ($p > 0.05$). Moreover, we detected that, in terms of the fungal burden in mice hearts, livers, spleens, lungs, and kidneys, all exhibited the same tendency to resist *C. albicans*; however, a dosage of 3.9 mg/kg CA may be the most effective for the treatment of OPC.

In addition, PAS staining demonstrated that the WT group mice possessed a complete tissue structure, with almost no fungus detected on their tongues. However, the control group mice were immunosuppressed with cortisone acetate and exhibited dense hyphal covering the dorsal layer of the mucosa; also, the superficial epithelial layer of the tongue was invaded by *C. albicans*, resulting in the destruction of the papillae and keratinized superficial epithelium. In contrast, the basal germinal layer was extensively proliferated, the tissue exhibited the tendency to repair, and only the superficial hyphal was reveled in mice treated with 3.9 mg/kg CA and FCZ (Fig. 9g). When tested in an experimental oral model of OPC, these data indicated that CA has a therapeutic effect in treating OPC in vivo, with 3.9 mg/kg CA being the optimal dosage observed.

Discussion

C. albicans is a type of symbiotic fungus that occurs in humans and can result in great physical and mental pain, as

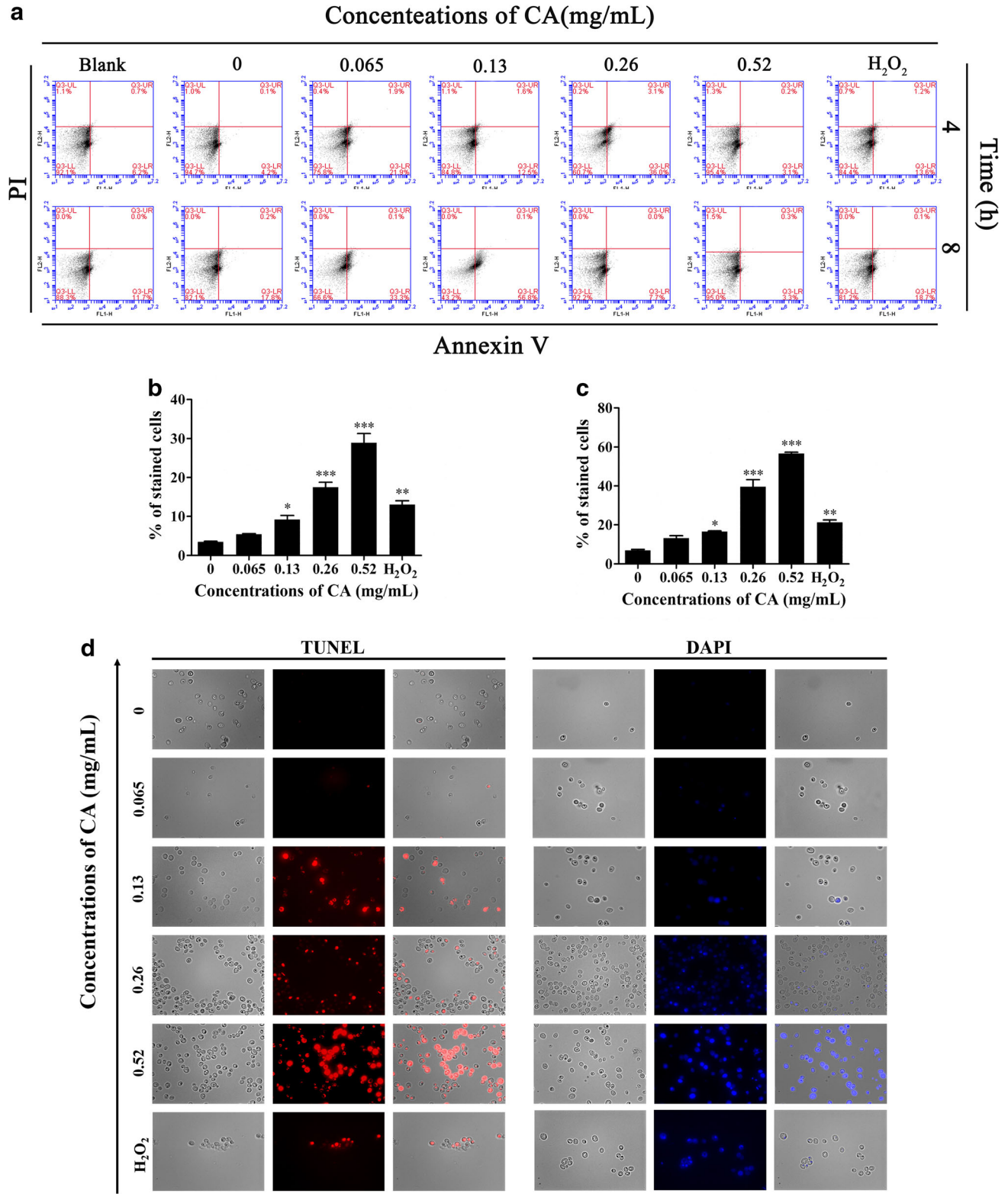

Fig. 7 Flow cytometry detected that the externalization of PS in *C. albicans* cells after exposure to CA. **A** The PS in *C. albicans* cells was analyzed using flow cytometry after the cells were treated with various concentrations of CA at 37 °C for 4 h and 8 h. **B** A one-way ANOVA of PS externalization after cells were treated with various concentrations of CA at 37 °C for 4 h. **C** Quantitative analysis of PS externalization after cells were treated with various concentrations of CA at 37 °C for 8 h. **D** TUNEL and DAPI staining were used to observe that damage and chromatin condensation that occurred in *C. albicans* cells after treatment by 0, 0.065, 0.13, 0.26, and 0.52 mg/mL CA. Red fluorescence means a positive signal in TUNEL staining and blue fluorescence means a nuclear signal after staining by DAPI. In all statistical analysis, $*p < 0.05$, $**p < 0.01$, and $***p < 0.001$, compared with the 0-mg/mL CA group

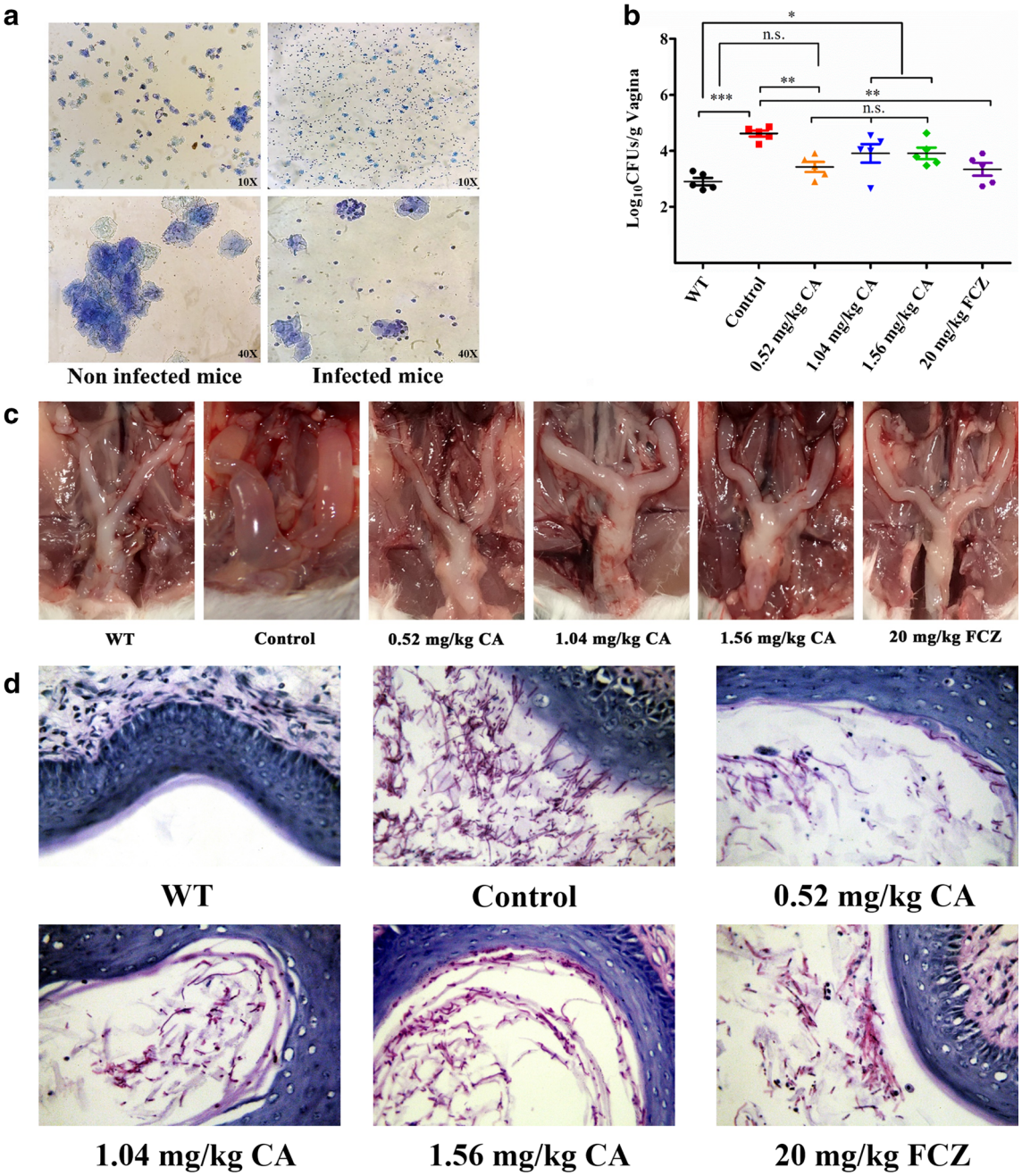

Fig. 8 CA improved the VVC invasion in vivo. **A** Diff-Quick straining was used to evaluate the murine model of VVC. **B** The fungal burden in mice vaginas; the vaginal was harvested, serially diluted, and plated for CFU counts; *$p < 0.05$, **$p < 0.01$, ***$p < 0.001$, and *n.s.* indicates that there was no significance. **C** The phenomenon in the uterus after becoming infected by *C. albicans* and treated by various concentrations of CA or FCZ. **D** PAS staining was used in every group to detect the colony of *C. albicans* in mice vaginas through a microscope, viewed at 40× magnification; a plum/purple stripe indicates the *C. albicans* hyphae

well as economic loss. *C. albicans* is considered one of the main pathogenic fungi that causes vaginitis and thrush (Fidel 2011). Similar to humans, mice who are infected with *C. albicans* also suffer from serious pain as a result of VVC and OPC. The weight and survival rate of mice experiencing OPC dramatically decline, and the presence of serious inflammation has been observed in a murine model of VVC (Figs. 8 and 9). Despite considerable advancements in *C. albicans* pathogenicity research and anti-fungus therapy, clinical fungal resistance is still a serious concern, and new mechanisms focusing on antifungal activity desperately require investigation. Previous research by our laboratory has attested that apoptosis and oxidative stress play important roles in the inhibition of fungi (Tian et al. 2017a; Tian et al. 2016).

Apoptosis is a form of strictly controlled cell death that reflects the death decision of cells in response to cues and is carried out by intrinsic cellular machinery (Degterev and Yuan 2008). Cancer cells are unique in that they are considered to be resistant to apoptosis, with the end goal of all chemotherapies being to directly or indirectly induce apoptosis (Burke 2017). Therefore, we wondered whether pathogen microorganisms that disrupt the stability of their host could also avoid this death by developing drug resistance to apoptosis, thus continuing to affect the health of the host.

Currently, peptaibols, anacardic acids, and amphotericin B are clinical antifungal agents that induce apoptosis (Muzaffar et al. 2016; Shi et al. 2012). Apoptosis has been considered as a promising method by which to manage fungal infections. In the current study, we identified that CA possessed the preferable anti-*C. albicans* effects under planktonic conditions, requiring a lower MIC of between 0.065 and 0.13 mg/mL when compared with other natural active ingredients, which have been reported in previous studies (Tian et al. 2017a, b). Like most antimicrobial agents, CA has been shown to enhance the ability of anti-biofilms in *C. albicans* and to decrease the expression of the gene HWP1. In addition, consistent with our Western blotting results (Fig. 4), after being treated by the encapsulated preparation of multilamellar liposome CA, they used fluorescence-activated cell sorting (FACS) detection to discover that cytochrome c was released into *C. albicans*' cytoplasm; however, the specific mechanisms of apoptosis introduced by CA remain unclear (Khan et al. 2017).

In a previous study, the morphology and ultrastructure of *C. albicans* cells were destroyed using CA, according to analysis by scanning electron micrograph and thin-section electron micrograph. Interestingly, we observed that, in the cells treated by CA, a large number of apoptosis bodies appeared in the images detected by thin-section electron micrograph, which the author in the previous study did not note; these results reinforce our findings (Taguchi et al. 2013). Thus, we decided to verify this interesting phenomenon and make clear the mechanism by which CA works against *C. albicans*.

ROS are byproducts of aerobic respiration, which, in their outer orbit, possess chemically reactive free radicals with one unpaired electron (Phaniendra et al. 2015). ROS award reactivity to various biological targets through their inherent chemical properties, including hydroxyl radicals (OH), hydrogen peroxide (H_2O_2), and superoxide anion (O_2^-), and are one of the main perpetrators connected with oxidative stress to introduce pathology by damaging lipids, proteins, and DNA, which have been deemed key biological hallmarks to apoptosis (Cross et al. 1987). The physiological production of ROS is caused by homeostatic metabolism, and low levels of ROS-introduced signaling could benefit cells. Nevertheless, the presence of high levels of ROS can bring about mitochondria damage, the destruction of organelle membranes, and even DNA breakage (Phaniendra et al. 2015). As such, the excessive accumulation of ROS can cause prolonged oxidative stress in cells, leading cells to senescent, undergo malignant transformation, and die by apoptosis.

The production of intracellular ROS was identified as one of the earliest changes implicated in apoptosis, and ROS-induced cell damage and programmed cell death has shown to be a frequent occurrence and normal antimicrobial mechanism in fungi of the *Aspergillus* species (Ben Yaakov et al. 2017; Tian et al. 2016). In this article, we detected that the accumulation of ROS in *C. albicans* is stimulated by CA, with the amount of ROS present increasing in accordance with the dose when compared to untreated cells (Fig. 2). In addition, part of the study indicated that the elevated levels of ROS may cause by the calcium concentration to rise in mitochondria, meaning that the relationship between the ROS and calcium can generate a positive feedback loop (Feissner et al. 2009). Furthermore, recent reports have demonstrated that an elevated mitochondrial membrane potential ($\Delta\psi_m$) relates to high intracellular ROS accumulation (Sukumar et al. 2016).

It has already been confirmed that the calcium ion plays a vital role in mediating programmed cell death, acting as a second principal intracellular messenger (Orrenius et al. 2003). Previous studies have indicated that calcium serves as an initiator of apoptosis in yeast when the intracellular calcium levels are enhanced and that calcium will move from intracellular stores into the cytoplasm when cells are in stress environments (Yun and Lee 2016). In our study, we have confirmed that the *C. albicans* cells were in a state of oxidative stress because of the excessive intracellular ROS accumulation when disposed by the various concentrations of CA (Fig. 2).

We then detected the calcium levels in the cytoplasm and mitochondria under when exposed to 0, 0.065, 0.13, 0.26, and 0.52 mg/mL CA. As shown in Fig. 3, as detected by flow cytometry and fluorescence microscope and evidenced by Rhod-2/AM and Fluo-3/AM fluorescent dyes, our data indicates that the calcium levels were all enhanced rapidly in the cytoplasm and mitochondria. In keeping with the findings of previous studies, calcium is a common mediator of apoptosis, calcium levels in the cytoplasm are similar to that in the nuclear and mitochondrial matrix in the stable circumstances. In addition, large amount of calcium was stored in other intracellular organelles such as endoplasmic reticulum (ER) which can accumulate calcium and contain a higher calcium level than the cytoplasm. When cells were stimulated by some exogenous pro-apoptotic agents, the calcium stores will be damaged and released a large number of calcium into cytoplasm (Bagur and Hajnoczky 2017; Swerdlow and Distelhorst 2007). Another research has reported that vacuole in yeast cells holds higher amounts of calcium than ER. Accordingly, the vacuole and ER may be the major source of calcium in *C. albicans* cytoplasm after treated by CA and then the calcium transfers from the cytoplasm to the mitochondria, leading

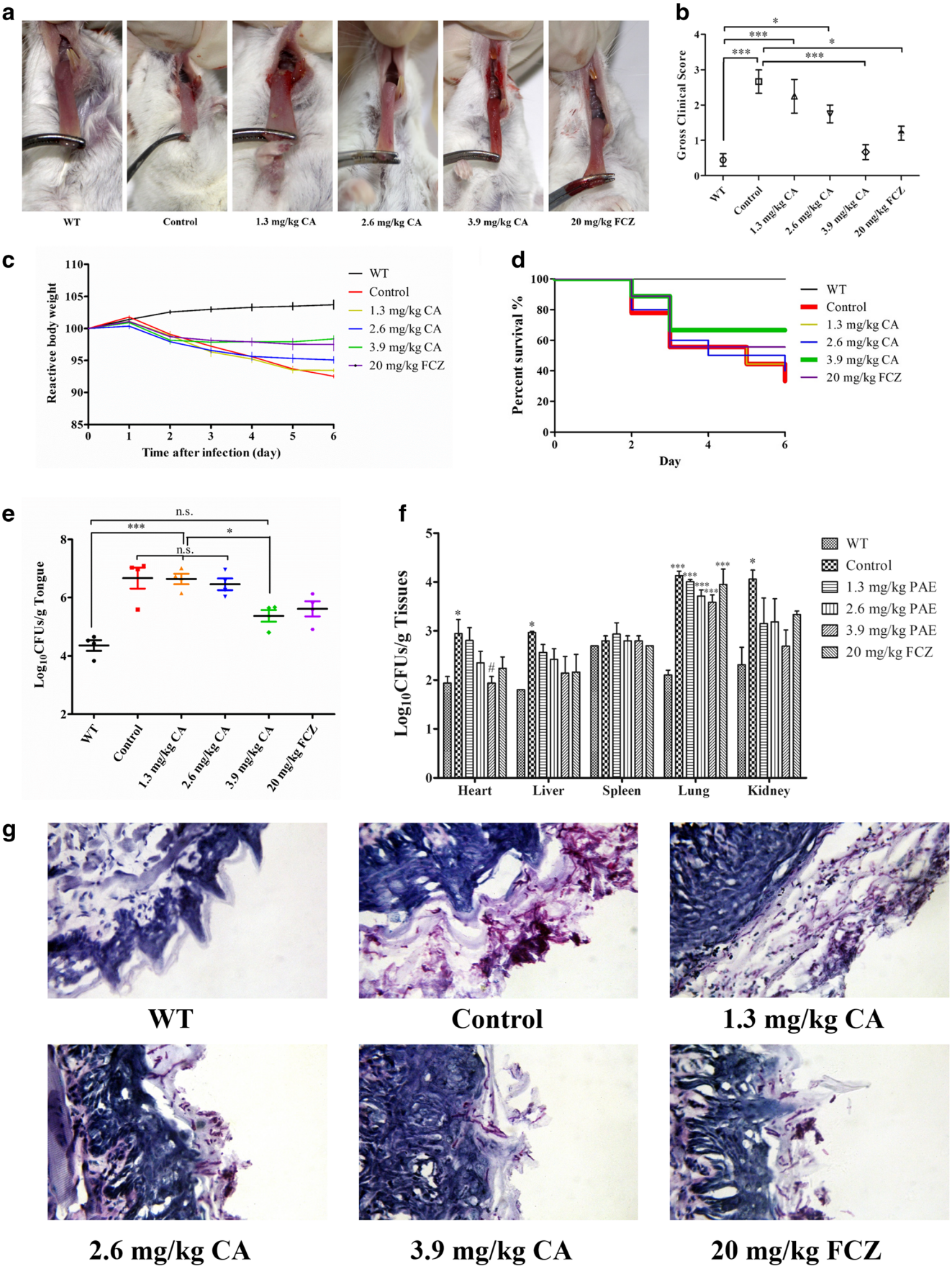
a
WT
Control
1.3 mg/kg CA
2.6 mg/kg CA
3.9 mg/kg CA
20 mg/kg FCZ
b
Gross Clinical Score
c
Reactivee body weight
Time after infection (day)
d
Percent survival %
Day
e
Log10CFUs/g Tongue
n.s.
f
Log10CFUs/g Tissues
Heart
Liver
Spleen
Lung
Kidney
1.3 mg/kg PAE
2.6 mg/kg PAE
3.9 mg/kg PAE
g
WT
Control
1.3 mg/kg CA
2.6 mg/kg CA
3.9 mg/kg CA
20 mg/kg FCZ

◀ **Fig. 9** CA was shown to be effective in treating OPC in the murine model. **A** Phenotypic evaluation of the colonization of *C. albicans* in infected mice and CA-treated mice tongues by visual analysis. **B** Clinical score of the *C. albicans* invasion area, indicating that CA has a treatment effect and prevents the diffusion of *C. albicans*. **C** The percentage of mice weight loss during the disease process. **D** After the invasion of *C. albicans*, CA enhanced the survival rate of mice. **E** The fungal burden in mice tongues was detected through harvested tissue, serially diluted, and plated for CFU counts. **F** Disseminated candidiasis was detected through mice viscera, such as the heart, liver, spleen, lung, and kidney, and evaluated using CFU counts. **G** PAS staining was used in every group to detect the colony of *C. albicans* in mice tongues through a microscope, viewed at 40× magnification; a plum/purple stripe indicates the *C. albicans* hyphae. In all statistical analysis, $*p < 0.05$, $***p < 0.001$, and *n.s.* indicates that it was not significant compared with the WT group; $^{\#}p < 0.05$, compared with CK group

to elevated levels of calcium in the mitochondria; the overload of calcium in the mitochondria can impair the function of mitochondria, cause mitochondrial membrane depolarization, and bring about pathological events such as apoptosis (Jou 2008; Yun and Lee 2016). An example of calcium concentrations becoming elevated in the mitochondria and inducing apoptosis is that of the case of *Saccharomyces cerevisiae* (Machida et al. 1998). Therefore, we next questioned whether intracellular ROS accumulation is affected by the elevation of the calcium concentration and whether the $\Delta\psi_m$ is affected by the ROS in *C. albicans* after treatment with CA.

$\Delta\psi_m$ plays a central role in many functions of organelles, and the most important function of $\Delta\psi_m$ is to propel adenosine triphosphate (ATP) synthesis through oxidative phosphorylation. Furthermore, $\Delta\psi_m$ is an evident marker of cellular energetics, as shown by its magnitude, set by equilibration between its production and expenditure through ATP synthesis and other dissipate processes (Logan et al. 2016). Related research now shows that the accumulation of ROS in the mitochondria is caused by an increase of $\Delta\psi_m$ in pathology and redox signaling (Murphy 2009). In addition, another report indicated that when stimulated by different signals, the damage of $\Delta\psi_m$ is a major cellular incident during apoptosis; apoptogenic factors will release from the mitochondria to the cytoplasm because of the disruption of $\Delta\psi_m$, leading to the opening of the transition pore of the mitochondrial membrane (Hwang et al. 2012).

Therefore, we used the JC-1 probe to measure the change of $\Delta\psi_m$ in *C. albicans* cells after being disposed by different concentrations of CA. JC-1 is an ideal fluorescent probe widely used to detect mitochondrial membrane potential ($\Delta\psi_m$). When the mitochondrial membrane potential is high, JC-1 aggregates in the matrix of the mitochondria to form a polymer that can produce red fluorescence; when the mitochondrial membrane potential is low, JC-1 cannot aggregate in the matrix of the mitochondria, and at this time, JC-1 is a monomer that produces green fluorescence. As shown in Fig. 4a and b, the $\Delta\psi_m$ was decreased obviously in the mitochondria after incubation with various concentrations of CA. Consistent with our conjecture, some studies have demonstrated that the $\Delta\psi_m$ decreased due to the increase of ATP production or thermogenesis, the dysfunction of the

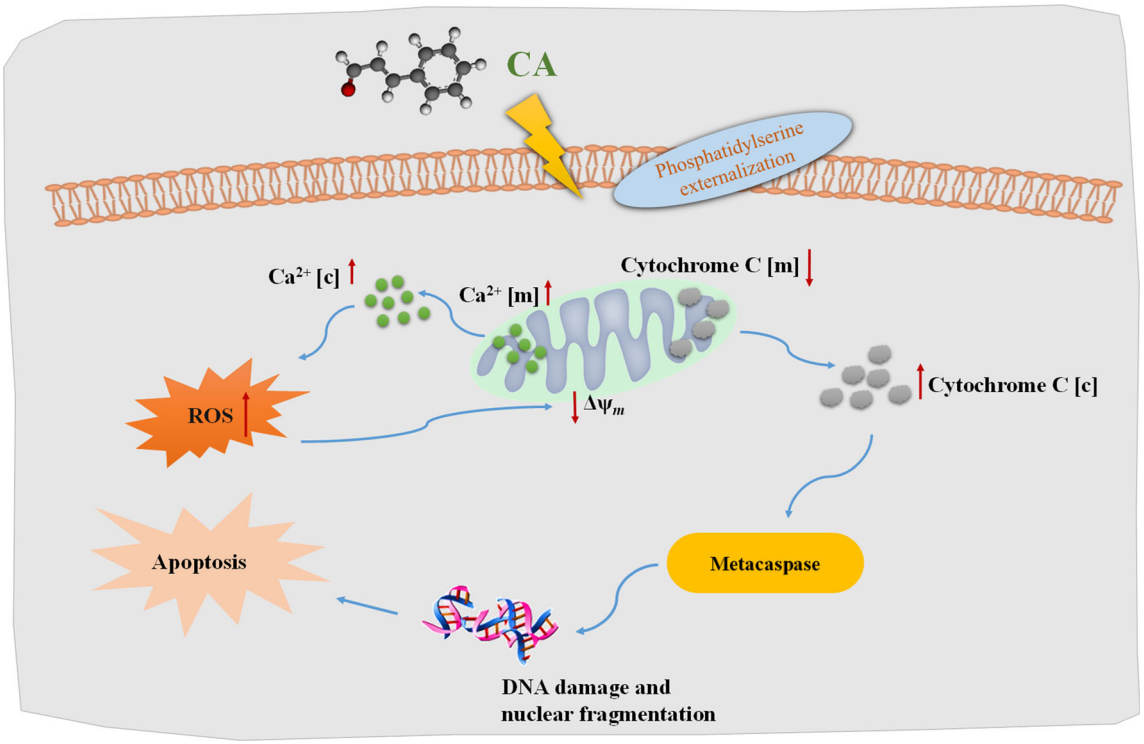

Fig. 10 A schematic illustration of the potential mechanism by which CA induces apoptosis in *C. albicans* cells to inhibit fungal growth

mitochondria, or programmed cell death (Yun et al. 2017). Based on our above results, the apoptosis induced by CA in *C. albicans* cells was obvious, and we also detected classic apoptosis factors in *C. albicans* such as cytochrome c and DNA damage.

Gottlieb et al. (2003))found that the decrease of Δψm mitochondria control matrix remodeling prior to the release of Cytochrome c. In our study, we detected that cytochrome c was released from the mitochondria to the cytoplasm using Western blotting in *C. albicans* cells after they were treated by CA (Fig. 5). The apoptosis occurred in cells requiring active downstream caspase, which necessitated the release of cytochrome c from the mitochondrial intermembrane space mediating the assembly of the apoptosome. Caspases were originally regarded as crucial markers of apoptosis (Yuan et al. 2016) and are members of the cysteine proteases, by they do not exist directly in yeast. However, previous reports have indicated that metacaspase coded by YAC1 was regarded as a neotype apoptotic target in yeast, plants, and protozoa (Cao et al. 2009). Our data shows that the metacaspase activities increased as CA concentrations increased after co-incubation in *C. albicans* cells (Fig. 6), suggesting that the cytochrome c transferred away from mitochondria can activate the metacaspase. Consistent with our previous speculations, the *C. albicans* cells exposed to CA lead to the increase of calcium levels in that cytoplasm and mitochondria, and Dong et al. have reported that the mitochondrial calcium uniporter will be activated which can sustain and increase the mitochondrial calcium intake when cells were stimulated by exogenous agents. And the sustained calcium uptake decreases respiratory functions and enlarges the accumulation of ROS in mitochondria matrix in a positive feedback manner (Demaurex and Rosselin 2017). The intracellular ROS to further accumulate and lead to the cytochrome c being released from the mitochondria to the cytoplasm, activating the metacaspase and resulting in apoptosis.

The activation of the caspase is responsible for the morphological and biochemical peculiarity of apoptosis, including phosphatidylserine exposure on the outer plasma membrane, DNA fragmentation, and the formation of apoptotic vesicles (Degterev et al. 2003). For clearer proof that *C. albicans* cells exhibited the characteristics of apoptosis, we measured the apoptosis markers. The recognition of exposed PS on programmed cell death cells is vital for their removal, and its translocation from the inner to the outer leaflet of the cytoplasmic membrane is an earlier indicator of apoptosis that can be detected using Annexin V-FITC fluorescence staining. As shown in Fig. 7a–c, our flow cytometry results indicated that CA caused PS externalization on the outer surface of the plasma membrane. Furthermore, according to a previous report, severe DNA damage is a result of apoptosis, and DNA damage and chromatin condensation are typical morphological features of a later period of apoptosis (Khoo et al. 2014). TUNEL staining is one of the most credible methods for the visual recognition of the amount of DNA fragmentation and chromatin condensation detected through a DAPI fluorescence probe. Our fluorescence results demonstrated that CA has a prominent effect on DNA damage and chromatin condensation in *C. albicans* cells (Fig. 7d).

Above all, our research indicates that in *C. albicans* cells, apoptosis is mediated by calcium and ROS changes after exposure to various concentrations of CA, and we propose a model for the apoptosis mechanism caused by CA in Fig. 10. In the preliminary stages of apoptosis, CA affects *C. albicans* cells' membrane plasm, resulting in the externalization of PS. We then observed that the intracellular levels of ROS and calcium were elevated. Because the cells undergo long-term stress, the augmentation of ROS and calcium promotes the release of cytoplasm C from the mitochondria to the cytoplasm and disturbs the steadiness of $\Delta\psi_m$, leading to an evident depolarization in $\Delta\psi_m$ and a destruction of the potential function of the mitochondrial membrane. Furthermore, we detected that the metacaspase was activated by various apoptosis factors to trigger the process of apoptosis, ultimately inducing the DNA damage and chromatin condensation.

Finally, we decided to confirm the actual therapeutic effect of topical therapy with CA in murine models of VVC and OPC. Our results indicated that CA possesses positive therapeutic effects in VVC and OPC and confirmed that the topical application of 0.52 mg/kg CA or 3.9 mg/kg CA can inhibit the development of VVC and OPC respectively. Nevertheless, the concentrations of 1.04 mg/kg CA and 1.56 mg/kg CA when treating VVC resulted in effects that were not so desirable, and we conjected that the high levels of CA inhibited the defense microbiota and change the micro-ecological environment in the vagina or introduced the cell death of mucosal cells in the host. Now, some researches have proved that defense bacteria and synergistic pathogens play the important role against monilial infection, we also want to verify these speculations by metagenomic sequencing and transcriptome sequencing in the future (Mukherjee et al. 2014; Xu et al. 2016; Yu et al. 2018). A recent study also showed that in the treatment of colitis, low concentrations of perillaldehyde have a better therapeutic effect, probably because the gut and vagina have their own unique microbiota (Uemura et al. 2018).

To our knowledge, CA has been reported to inhibit neointimal hyperplasia through the activation of NRF2. Another report also indicated that CA prohibits ubiquitination with the upregulation of cytoprotective NRF2 genes and enhances cellular glutathione in colorectal cancer (Buglak et al. 2018; Long et al. 2015). In

addition, CA has been demonstrated to possess the capacity to anesis the symptoms of cardiac inflammation and fibrosis by suppressing the activation of NLRP3 inflammasome, which was introduced by attenuating CD36-mediated TLR4/6-IRAK4/1 signaling. CA has also been reported to improve permanent cerebral ischemia injuries by reducing the expression of toll-like reporter 4 and the nuclear translocation of NF-κB (Kang et al. 2016; Zhao et al. 2015). Similar to its effect on inflammatory diseases, the mechanisms by which CA resists OPC and VVC are still unclear. As such, detailed investigations are needed to make clear the mechanisms by which OPC and VVC are treated by CA at the molecular level.

In conclusion, we identified the MIC of CA in treating *C. albicans* and demonstrated that low concentrations of CA are efficient to introduce apoptosis in vitro, mediated by intracellular calcium and ROS accumulation and inducing a series apoptosis factors that lead to mitochondrial dysfunction through the metacaspase pathway. CA also exhibited a little better pro-apoptosis effect than H_2O_2. Finally, demonstrations of the treatment of OPC and VVC by CA corroborate that this molecule is a promising potential candidate as an antifungal agent for the treatment of *C. albicans* invasion.

Authors' contributions JT and XP designed the experiments. LC, ZW, and LL performed the experiments. SQ and YM analyzed the data. LC and YL drafted the manuscript. All authors read and approved the final manuscript.

Funding information This study was funded by National Natural Science Foundation of China (31972171, 31671944, 31570028), Six Talent Peaks Project of Jiangsu Province (SWYY-026), Qing Lan Project of Jiangsu Province, Natural Science Foundation by Xuzhou City (KC17053), Jiangsu Science and Technology Agency Project (BK20141148) and the PAPD of Jiangsu Higher Education Institutions.

Compliance with ethical standards

Ethical approval All animal or human experiments in this study were performed in strict accordance with the Guide for the Care and Use of Chinese legislation, the Ministry of Science and Technology of China and were approved by the Institutional Jiangsu Normal University Committee for Animal Experiments.

Competing interests The authors declare that they have no competing interests.

References

Aguirre J, Rios-Momberg M, Hewitt D, Hansberg W (2005) Reactive oxygen species and development in microbial eukaryotes. Trends Microbiol 13(3):111–118. https://doi.org/10.1016/j.tim.2005.01.007

Alonso-Monge R, Carvaihlo S, Nombela C, Rial E, Pla J (2009) The hog1 MAP kinase controls respiratory metabolism in the fungal pathogen *Candida albicans*. Microbiology 155(Pt 2):413–423. https://doi.org/10.1099/mic.0.023309-0

Atanasov AG, Waltenberger B, Pferschy-Wenzig EM, Linder T, Wawrosch C, Uhrin P, Temml V, Wang L, Schwaiger S, Heiss EH, Rollinger JM, Schuster D, Breuss JM, Bochkov V, Mihovilovic MD, Kopp B, Bauer R, Dirsch VM, Stuppner H (2015) Discovery and resupply of pharmacologically active plant-derived natural products: a review. Biotechnol Adv 33(8):1582–1614. https://doi.org/10.1016/j.biotechadv.2015.08.001

Bagur R, Hajnoczky G (2017) Intracellular Ca^{2+} sensing: its role in calcium homeostasis and signaling. Mol Cell 66(6):780–788. https://doi.org/10.1016/j.molcel.2017.05.028

Ben Yaakov D, Shadkchan Y, Albert N, Kontoyiannis DP, Osherov N (2017) The quinoline bromoquinol exhibits broad-spectrum antifungal activity and induces oxidative stress and apoptosis in *Aspergillus fumigatus*. J Antimicrob Chemother 72(8):2263–2272. https://doi.org/10.1093/jac/dkx117

Brown GD, Denning DW, Gow NA, Levitz SM, Netea MG, White TC (2012) Hidden killers: human fungal infections. Sci Transl Med 4(165):165rv13. https://doi.org/10.1126/scitranslmed.3004404

Buglak NE, Jiang W, Bahnson ESM (2018) Cinnamic aldehyde inhibits vascular smooth muscle cell proliferation and neointimal hyperplasia in zucker diabetic fatty rats. Redox Biol 19:166–178. https://doi.org/10.1016/j.redox.2018.08.013

Burke PJ (2017) Mitochondria, bioenergetics and apoptosis in cancer. Trends Cancer 3(12):857–870. https://doi.org/10.1016/j.trecan.2017.10.006

Burt SA, Adolfse SJM, Ahad DSA, Tersteeg-Zijderveld MHG, Jongerius-Gortemaker BGM, Post JA, Bruggemann H, Santos RR (2016) Cinnamaldehyde, carvacrol and organic acids affect gene expression of selected oxidative stress and inflammation markers in ipec-j2 cells exposed to salmonella typhimurium. Phytother Res 30(12):1988–2000. https://doi.org/10.1002/ptr.5705

Cao YY, Huang S, Dai BD, Zhu ZY, Lu H, Dong LL, Cao YB, Wang Y, Gao PH, Chai YF, Jiang YY (2009) *Candida albicans* cells lacking camca1-encoded metacaspase show resistance to oxidative stress-induced death and change in energy metabolism. Fungal Genet Biol 46(2):183–189. https://doi.org/10.1016/j.fgb.2008.11.001

Conti HR, Shen F, Nayyar N, Stocum E, Sun JN, Lindemann MJ, Ho AW, Hai JH, Yu JJ, Jung JW, Filler SG, Masso-Welch P, Edgerton M, Gaffen SL (2009) Th17 cells and IL-17 receptor signaling are essential for mucosal host defense against oral candidiasis. J Exp Med 206(2):299–311. https://doi.org/10.1084/jem.20081463

Cross CE, Halliwell B, Borish ET, Pryor WA, Ames BN, Saul RL, McCord JM, Harman D (1987) Oxygen radicals and human disease. Ann Intern Med 107(4):526–545

Degterev A, Yuan J (2008) Expansion and evolution of cell death programmes. Nat Rev Mol Cell Biol 9(5):378–390. https://doi.org/10.1038/nrm2393

Degterev A, Boyce M, Yuan J (2003) A decade of caspases. Oncogene 22(53):8543–8567. https://doi.org/10.1038/sj.onc.1207107

Demaurex N, Rosselin M (2017) Redox control of mitochondrial calcium uptake. Mol Cell 65(6):961–962. https://doi.org/10.1016/j.molcel.2017.02.029

Feissner RF, Skalska J, Gaum WE, Sheu SS (2009) Crosstalk signaling between mitochondrial Ca^{2+} and ROS. Front Biosci-Landmrk 14:1197–1218. https://doi.org/10.2741/3303

Fidel PL Jr (2011) Candida-host interactions in HIV disease: implications for oropharyngeal candidiasis. Adv Dent Res 23(1):45–49. https://doi.org/10.1177/0022034511399284

Fuchs Y, Steller H (2011) Programmed cell death in animal development and disease. Cell 147(4):742–758. https://doi.org/10.1016/j.cell.2011.10.033

Giacomello M, Drago I, Pizzo P, Pozzan T (2007) Mitochondrial Ca^{2+} as a key regulator of cell life and death. Cell Death Differ 14(7):1267–1274. https://doi.org/10.1038/sj.cdd.4402147

Gottlieb E, Armour SM, Harris MH, Thompson CB (2003) Mitochondrial membrane potential regulates matrix configuration and cytochrome c release during apoptosis. Cell Death Differ 10(6):709–717. https://doi.org/10.1038/sj.cdd.4401231

Hise AG, Tomalka J, Ganesan S, Patel K, Hall BA, Brown GD, Fitzgerald KA (2009) An essential role for the NLRP3 inflammasome in host defense against the human fungal pathogen *Candida albicans*. Cell Host Microbe 5(5):487–497. https://doi.org/10.1016/j.chom.2009.05.002

Hwang JH, Hwang IS, Liu QH, Woo ER, Lee DG (2012) Medioresinol leads to intracellular ROS accumulation and mitochondria-mediated apoptotic cell death in *Candida albicans*. Biochimie 94(8):1784–1793. https://doi.org/10.1016/j.biochi.2012.04.010

Jou MJ (2008) Pathophysiological and pharmacological implications of mitochondria-targeted reactive oxygen species generation in astrocytes. Adv Drug Deliv Rev 60(13–14):1512–1526. https://doi.org/10.1016/j.addr.2008.06.004

Kang LL, Zhang DM, Ma CH, Zhang JH, Jia KK, Liu JH, Wang R, Kong LD (2016) Cinnamaldehyde and allopurinol reduce fructose-induced cardiac inflammation and fibrosis by attenuating CD36-mediated TLR4/6-IRAK4/1 signaling to suppress NLRP3 inflammasome activation. Sci Rep 6:27460. https://doi.org/10.1038/srep27460

Khan SN, Khan S, Iqbal J, Khan R, Khan AU (2017) Enhanced killing and antibiofilm activity of encapsulated cinnamaldehyde against *Candida albicans*. Front Microbiol 8:1641. https://doi.org/10.3389/fmicb.2017.01641

Khoo KH, Verma CS, Lane DP (2014) Drugging the p53 pathway: understanding the route to clinical efficacy. Nat Rev Drug Discov 13(3):217–236. https://doi.org/10.1038/nrd4236

Kuang S, Liu G, Cao R, Zhang L, Yu Q, Sun C (2017) Mansouramycin C kills cancer cells through reactive oxygen species production mediated by opening of mitochondrial permeability transition pore. Oncotarget 8(61):104057–104071. https://doi.org/10.18632/oncotarget.22004

Liao JC, Deng JS, Chiu CS, Hou WC, Huang SS, Shie PH, Huang GJ (2012) Anti-inflammatory activities of cinnamomum cassia constituents *in vitro* and *in vivo*. Evid Based Complement Alternat Med 2012:429320–429312. https://doi.org/10.1155/2012/429320

Logan A, Pell VR, Shaffer KJ, Evans C, Stanley NJ, Robb EL, Prime TA, Chouchani ET, Cocheme HM, Fearnley IM, Vidoni S, James AM, Porteous CM, Partridge L, Krieg T, Smith RAJ, Murphy MP (2016) Assessing the mitochondrial membrane potential in cells and *in vivo* using targeted click chemistry and mass spectrometry. Cell Metab 23(2):379–385. https://doi.org/10.1016/j.cmet.2015.11.014

Long M, Tao S, Rojo de la Vega M, Jiang T, Wen Q, Park SL, Zhang DD, Wondrak GT (2015) Nrf2-dependent suppression of azoxymethane/dextran sulfate sodium-induced colon carcinogenesis by the cinnamon-derived dietary factor cinnamaldehyde. Cancer Prev Res (Phila) 8(5):444–454. https://doi.org/10.1158/1940-6207.CAPR-14-0359

Machida K, Tanaka T, Fujita K, Taniguchi M (1998) Farnesol-induced generation of reactive oxygen species via indirect inhibition of the mitochondrial electron transport chain in the yeast Saccharomyces cerevisiae. J Bacteriol 180(17):4460–4465

Madeo F, Frohlich E, Frohlich KU (1997) A yeast mutant showing diagnostic markers of early and late apoptosis. J Cell Biol 139(3):729–734

Madeo F, Frohlich E, Ligr M, Grey M, Sigrist SJ, Wolf DH, Frohlich KU (1999) Oxygen stress: a regulator of apoptosis in yeast. J Cell Biol 145(4):757–767

Mukherjee PK, Chandra J, Retuerto M, Sikaroodi M, Brown RE, Jurevic R, Salata RA, Lederman MM, Gillevet PM, Ghannoum MA (2014) Oral mycobiome analysis of HIV-infected patients: identification of *Pichia* as an antagonist of opportunistic fungi. PLoS Pathog 10(3):e1003996. https://doi.org/10.1371/journal.ppat.1003996

Murphy MP (2009) How mitochondria produce reactive oxygen species. Biochem J 417:1–13. https://doi.org/10.1042/Bj20081386

Muzaffar S, Bose C, Banerji A, Nair BG, Chattoo BB (2016) Anacardic acid induces apoptosis-like cell death in the rice blast fungus *Magnaporthe oryzae*. Appl Microbiol Biotechnol 100(1):323–335. https://doi.org/10.1007/s00253-015-6915-4

Nucci M, Queiroz-Telles F, Alvarado-Matute T, Tiraboschi IN, Cortes J, Zurita J, Guzman-Blanco M, Santolaya ME, Thompson L, Sifuentes-Osornio J, Echevarria JI, Colombo AL, Latin American Invasive Mycosis N (2013) Epidemiology of candidemia in Latin America: a laboratory-based survey. PLoS One 8(3):e59373. https://doi.org/10.1371/journal.pone.0059373

Orrenius S, Zhivotovsky B, Nicotera P (2003) Regulation of cell death: the calcium-apoptosis link. Nat Rev Mol Cell Biol 4(7):552–565. https://doi.org/10.1038/nrm1150

Phaniendra A, Jestadi DB, Periyasamy L (2015) Free radicals: properties, sources, targets, and their implication in various diseases. Indian J Clin Biochem 30(1):11–26. https://doi.org/10.1007/s12291-014-0446-0

Phillips AJ, Sudbery I, Ramsdale M (2003) Apoptosis induced by environmental stresses and amphotericin B in Candida albicans. Proc Natl Acad Sci U S A 100(24):14327–14332. https://doi.org/10.1073/pnas.2332326100

Qu S, Chen L, Tian H, Wang Z, Wang F, Wang L, Li J, Ji H, Xi L, Feng Z, Tian J, Feng Z (2019) Effect of perillaldehyde on prophylaxis and treatment of vaginal candidiasis in a murine model. Front Microbiol 10:1466. https://doi.org/10.3389/fmicb.2019.01466

Sawicki R, Golus J, Przekora A, Ludwiczuk A, Sieniawska E, Ginalska G (2018) Antimycobacterial activity of cinnamaldehyde in a *Mycobacterium tuberculosis*(H37Ra) model. Molecules 23(9). https://doi.org/10.3390/molecules23092381

Shi M, Chen L, Wang XW, Zhang T, Zhao PB, Song XY, Sun CY, Chen XL, Zhou BC, Zhang YZ (2012) Antimicrobial peptaibols from *Trichoderma pseudokoningii* induce programmed cell death in plant fungal pathogens. Microbiology 158(Pt 1):166–175. https://doi.org/10.1099/mic.0.052670-0

Sobel JD (2007) Vulvovaginal candidosis. Lancet 369(9577):1961–1971. https://doi.org/10.1016/S0140-6736(07)60917-9

Solis NV, Swidergall M, Bruno VM, Gaffen SL, Filler SG (2017) The aryl hydrocarbon receptor governs epithelial cell invasion during oropharyngeal candidiasis. MBio 8(2). https://doi.org/10.1128/mBio.00025-17

Sukumar M, Liu J, Mehta GU, Patel SJ, Roychoudhuri R, Crompton JG, Klebanoff CA, Ji Y, Li P, Yu Z, Whitehill GD, Clever D, Eil RL, Palmer DC, Mitra S, Rao M, Keyvanfar K, Schrump DS, Wang E, Marincola FM, Gattinoni L, Leonard WJ, Muranski P, Finkel T, Restifo NP (2016) Mitochondrial membrane potential identifies cells with enhanced stemness for cellular therapy. Cell Metab 23(1):63–76. https://doi.org/10.1016/j.cmet.2015.11.002

Swerdlow S, Distelhorst CW (2007) Bcl-2-regulated calcium signals as common mediators of both apoptosis and autophagy. Dev Cell 12(2):178–179. https://doi.org/10.1016/j.devcel.2007.01.008

Taguchi Y, Hasumi Y, Abe S, Nishiyama Y (2013) The effect of cinnamaldehyde on the growth and the morphology of *Candida albicans*. Med Mol Morphol 46(1):8–13. https://doi.org/10.1007/s00795-012-0001-0

Tian J, Wang Y, Lu Z, Sun C, Zhang M, Zhu A, Peng X (2016) Perillaldehyde, a promising antifungal agent used in food preservation, triggers apoptosis through a metacaspase-dependent pathway in *Aspergillus flavus*. J Agric Food Chem 64(39):7404–7413. https://doi.org/10.1021/acs.jafc.6b03546

Tian H, Qu S, Wang Y, Lu Z, Zhang M, Gan Y, Zhang P, Tian J (2017a) Erratum to: calcium and oxidative stress mediate perillaldehyde-induced apoptosis in *Candida albicans*. Appl Microbiol Biotechnol 101(8):3347–3348. https://doi.org/10.1007/s00253-017-8217-5

Tian J, Lu Z, Wang Y, Zhang M, Wang X, Tang X, Peng X, Zeng H (2017b) Nerol triggers mitochondrial dysfunction and disruption via elevation of Ca^{2+} and ROS in *Candida albicans*. Int J Biochem Cell Biol 85:114–122. https://doi.org/10.1016/j.biocel.2017.02.006

Tian J, Gan Y, Pan C, Zhang M, Wang X, Tang X, Peng X (2018) Nerol-induced apoptosis associated with the generation of ROS and Ca^{2+} overload in saprotrophic fungus *Aspergillus flavus*. Appl Microbiol Biotechnol 102(15):6659–6672. https://doi.org/10.1007/s00253-018-9125-z

Uemura T, Yashiro T, Oda R, Shioya N, Nakajima T, Hachisu M, Kobayashi S, Nishiyama C, Arimura GI (2018) Intestinal anti-inflammatory activity of perillaldehyde. J Agric Food Chem 66(13):3443–3448. https://doi.org/10.1021/acs.jafc.8b00353

Utchariyakiat I, Surassmo S, Jaturanpinyo M, Khuntayaporn P, Chomnawang MT (2016) Efficacy of cinnamon bark oil and cinnamaldehyde on anti-multidrug resistant *Pseudomonas aeruginosa* and the synergistic effects in combination with other antimicrobial agents. BMC Complement Altern Med 16:158. https://doi.org/10.1186/s12906-016-1134-9

Wang C, Youle RJ (2009) The role of mitochondria in apoptosis. Annu Rev Genet 43:95–118. https://doi.org/10.1146/annurev-genet-102108-134850

Wisplinghoff H, Bischoff T, Tallent SM, Seifert H, Wenzel RP, Edmond MB (2004) Nosocomial bloodstream infections in US hospitals: analysis of 24,179 cases from a prospective nationwide surveillance study. Clin Infect Dis 39(3):309–317. https://doi.org/10.1086/421946

Xu H, Sobue T, Bertolini M, Thompson A, Dongari-Bagtzoglou A (2016) *Streptococcus oralis* and *Candida albicans* synergistically activate mu-calpain to degrade E-cadherin from oral epithelial junctions. J Infect Dis 214(6):925–934. https://doi.org/10.1093/infdis/jiw201

Youn HS, Lee JK, Choi YJ, Saitoh SI, Miyake K, Hwang DH, Lee JY (2008) Cinnamaldehyde suppresses toll-like receptor 4 activation mediated through the inhibition of receptor oligomerization. Biochem Pharmacol 75(2):494–502. https://doi.org/10.1016/j.bcp.2007.08.033

Yu XY, Fu F, Kong WN, Xuan QK, Wen DH, Chen XQ, He YM, He LH, Guo J, Zhou AP, Xi YH, Ni LJ, Yao YF, Wu WJ (2018) *Streptococcus agalactiae* inhibits *Candida albicans* hyphal development and diminishes host vaginal mucosal TH17 response. Front Microbiol 9:198. https://doi.org/10.3389/fmicb.2018.00198

Yuan J, Najafov A, Py BF (2016) Roles of caspases in necrotic cell death. Cell 167(7):1693–1704. https://doi.org/10.1016/j.cell.2016.11.047

Yun DG, Lee DG (2016) Silibinin triggers yeast apoptosis related to mitochondrial Ca^{2+} influx in *Candida albicans*. Int J Biochem Cell Biol 80:1–9. https://doi.org/10.1016/j.biocel.2016.09.008

Yun X, Rao W, Xiao C, Huang Q (2017) Apoptosis of leukemia K562 and Molt-4 cells induced by emamectin benzoate involving mitochondrial membrane potential loss and intracellular Ca^{2+} modulation. Environ Toxicol Pharmacol 52:280–287. https://doi.org/10.1016/j.etap.2017.04.013

Zaoutis TE, Argon J, Chu J, Berlin JA, Walsh TJ, Feudtner C (2005) The epidemiology and attributable outcomes of candidemia in adults and children hospitalized in the United States: a propensity analysis. Clin Infect Dis 41(9):1232–1239. https://doi.org/10.1086/496922

Zhao J, Zhang X, Dong L, Wen Y, Zheng X, Zhang C, Chen R, Zhang Y, Li Y, He T, Zhu X, Li L (2015) Cinnamaldehyde inhibits inflammation and brain damage in a mouse model of permanent cerebral ischaemia. Br J Pharmacol 172(20):5009–5023. https://doi.org/10.1111/bph.13270